IN-92-TM
106529
P.55

554-FDD-91/004
CSC/TM-91/6008

Future Mission Studies

Preliminary Comparisons of Solar Flux Models

December 1991

(NASA-TM-107947) FUTURE MISSION STUDIES: PRELIMINARY COMPARISONS OF SOLAR FLUX MODELS (NASA) 55 p
N92-28869
Unclas
G3/92 0106529

National Aeronautics and
Space Administration

Goddard Space Flight Center
Flight Dynamics Division / Code 550
Greenbelt, Maryland 20771

554-FDD-91/004
CSC/TM-91/6008

FUTURE MISSION STUDIES

PRELIMINARY COMPARISONS OF SOLAR FLUX MODELS

ORIGINAL CONTAINS
COLOR ILLUSTRATIONS

December 1991

FLIGHT DYNAMICS DIVISION

CODE 550

Developed Under
the Direction of

J. Cooley/M. Saltzberg
GSFC/Code 554

Through

L. Roszman
Task 404
Contract NAS 5-31500
Computer Sciences Corporation

554-FDD-91/004
CSC/TM-91/6008

FUTURE MISSION STUDIES

PRELIMINARY COMPARISONS OF SOLAR FLUX MODELS

December 1991

The primary contributor to this document is

S. Ashrafi CSC

APPROVED FOR PUBLICATION BY:

James Cooley / J. A. Jackson for
J. Cooley/M. Saltzberg,
ATRs
Flight Dynamics Analysis
Branch

Mina V. Samii
M. Samii, Manager
Orbit Analysis Department

PAGE 11 INTENTIONALLY BLANK

3

PRECEDING PAGE BLANK NOT FILMED

ABSTRACT

The purpose of this document is to present the results of comparisons of the solar flux models. (The wavelength λ = 10.7 cm radio flux is the best indicator of the strength of the ionizing radiations such as solar ultraviolet and x-ray emissions that directly affect the atmospheric density thereby changing the orbit lifetime of satellites. Thus, accurate forecasting of solar flux $F_{10.7}$ is crucial for orbit determination of spacecrafts.) The measured solar flux recorded by National Oceanic and Atmospheric Administration (NOAA) is compared against the forecasts made by Schatten, Marshall Space Flight Center (MSFC), and NOAA itself. This document also discusses the possibility of a combined linear, unbiased minimum-variance estimation that properly combines all three models into one that minimizes the variance. All the physics inherent in each model are combined. This is considered to be the dead-end statistical approach to solar flux forecasting before any nonlinear chaotic approach.

The research for this document was completed in December 1990.

6176

PAGE iv INTENTIONALLY BLANK

PRECEDING PAGE BLANK NOT FILMED

TABLE OF CONTENTS

Section 1 - Introduction 1-1

Section 2 - Solar Flux $F_{10.7}$ Prediction. 2-1

2.1 Mathematical Perspectives 2-1
2.2 Graphical Analysis of Data. 2-1
2.3 Description of Graphs 2-2

Section 3 - Statistical Analysis 3-1

3.1 Check of a Hypothesis 3-1
3.2 Chi-Square Distribution 3-3

Section 4 - Linear, Unbiased Minimum-Variance Estimation (LUMVE) 4-1

4.1 Mathematical Formulation. 4-1
4.2 Graphical Analysis of Data. 4-5

Section 5 - Conclusions and Recommendations. 5-1

References

PAGE IV INTENTIONALLY BLANK

PRECEDING PAGE BLANK NOT FILMED

LIST OF ILLUSTRATIONS

Figure

2-1 Plot of Solar Flux Values and Schatten Nominal, +2 Sigma, and -2 Sigma Predictions (May 1990). 2-3

2-2 Plot of Solar Flux Values, Schatten Nominal Prediction, and NOAA 27-Day Nominal Predictions (May 1990). 2-4

2-3 Plot of Solar Flux Values, Schatten Nominal and -2 Sigma Predictions, and NOAA 27-Day Nominal Predictions (May 1990). 2-5

2-4 Plot of Solar Flux Values Minus the Mean Value Normalized by Standard Deviation (May 1990). 2-6

2-5 Plot of Solar Flux Values and the Schatten Nominal, +2 Sigma, and -2 Sigma Predictions (June 1990) 2-7

2-6 Plot of Solar Flux Values and the Schatten Nominal, -2 Sigma Predictions, and the NOAA 27-Day Nominal Predictions (June 1990) 2-8

2-7 Plot of Solar Flux Values and the Schatten Nominal, +2 Sigma, and -2 Sigma Predictions (July 1990) 2-9

2-8 Plot of Solar Flux Values, the Schatten Nominal, -2 Sigma Predictions, and the NOAA 27-Day Nominal Predictions (July 1990) 2-10

2-9 Plot of Solar Flux Values and the Schatten Nominal, -2 Sigma, and +2 Sigma Predictions (August 1990) 2-11

2-10 Plot of Solar Flux Values, the Schatten Nominal, -2 Sigma, and NOAA 27-Day Nominal Predictions (August 1990) 2-12

2-11 Plot of Actual NOAA Solar Flux Values for October 15, 1988, to September 17, 1990 . . 2-13

2-12 Plot of Actual Solar Flux Values and Mean Value. 2-14

2-13 Plot of Solar Flux Values and the Nominal Best Schatten and MSFC Predictions. 2-15

2-14 Plot of Solar Flux Values, the Schatten Nominal and +2 Sigma Predictions, and the MSFC Nominal and 97.7 Percent Predictions 2-16

LIST OF ILLUSTRATIONS (Cont'd)

Figure

2-15 Plot of the Nominal Schatten and MSFC 95-Percent Predictions Confidence Interval and the Average of the Actual Solar Flux Values 2-17

2-16 Plot of the Schatten +2 Sigma and MSFC 97.7-Percent Predictions Confidence Interval and the Average of the Actual Solar Flux Values 2-18

2-17 Plot of Actual Solar Flux Values From October 15, 1988, to September 17, 1990, and the Best Nominal Schatten and MSFC Prediction With the 30-Day Partitioned Average of Actual Solar Flux Values 2-19

2-18 Plot of the Actual Solar Flux Values for a Different Timespan (MJD 13400 to 15200) 2-20

2-19 Plot of the Actual Solar Flux Values and Its Average for a Different Timespan (MJD 15000 to 16800). 2-21

4-1 Calculation of the Parameters Used in Linear, Unbiased Minimum-Variance Estimation (Running Procedure: Running Average of Data). 4-7

4-2 Predicted Flux by NOAA, MSFC, Schatten (Nominals) and the Result of Linear, Unbiased Minimum-Variance Estimation (Time Evolution of the Coefficients a_n, a_m, and a_s--Running Procedure). 4-8

4-3 Calculation of the Parameters Used in Linear, Unbiased Minimum-Variance Estimation (6-Month Partition Procedure--Partitioned Average of Data) . . 4-9

4-4 Plot of the Predicted Flux by NOAA, MSFC, Schatten (Nominal) and Result of Linear, Unbiased Minimum-Variance Estimation (Time Evolution of the Coefficients a_n, a_m, and a_s--Partitioned Procedure). . . 4-9

4-5 Plot of the Actual Solar Flux Values, Nominal Schatten and MSFC Predictions, and 81-Day Average. 4-10

4-6 Plot of the Actual Solar Flux Values, Schatten, and MSFC Predictions With 30-Day Running Average and 30-Day Partitioned Average 4-11

LIST OF ILLUSTRATIONS (Cont'd)

Figure

4-7 Plot of the Actual Solar Flux Values, Schatten, MSFC Predictions, and 81-Day Average With 30-Day Running Average and 30-Day Partitioned Average. . . 4-12

4-8 Plot of the Actual Solar Flux Values, Schatten, and MSFC Predictions (30-Day Running Average; 30-Day Partitioned Average; and Linear, Unbiased Minimum-Variance Estimation by 6-Month Partitioned Procedure). 4-13

4-9 Plot of the Actual Solar Flux Values and the Schatten and MSFC Predictions With 30-Day Running Average and the Estimated Combined Flux With Partitioned Procedure. . 4-14

4-10 Plot of the Nominal Schatten, MSFC, and NOAA Minus 30-Day Average of Actual Values and Linear, Unbiased Minimum-Variance Estimation (Normalized). 4-15

SECTION 1 - INTRODUCTION

This document is the first part of a sequence of preliminary studies of solar flux observed at the wavelength λ = 10.7 cm range. The sequence starts with comparisons of different solar flux models and gradually leads to a critical stochastic approach, which further produces a geometric approach to the prediction of chaotic solar flux time series.

The analysis in this first sequence is based on the available forecasts by Schatten (at Goddard Space Flight Center (GSFC)) (Reference 1), Marshall Space Flight Center (MSFC) (Reference 2), and National Oceanic and Atmospheric Administration (NOAA) (Reference 3). The comparisons are made against actual observed values that are collected by NOAA (Reference 3).

The observable radio spectrum extends from 1 centimeter (cm) to 10 meters (m). Like the optical spectrum, the radio spectrum is limited on its short wavelength end by absorption in the Earth's atmosphere (by molecules of oxygen and water vapor). On the long wavelength end, the lower atmosphere is always transparent, even on cloudy days. But a high layer, called the ionosphere, begins to interfere at around λ = 10 m (References 4 and 5).

The radio waves are radiated by fast-moving electrons in the highly ionized gases of the outer solar atmosphere. Ionized gases, which are fully transparent to visible light, however, may be opaque to radio waves at certain wavelengths. The opacity depends on the density of ionized gas. In the solar chromosphere, where density is high, the gases are completely opaque to meter wavelengths; only the centimeter waves can escape the Sun to reach the Earth. The Sun that is observed is only the visible Sun; it appears larger in the radio region (that is, the appearance dimension is proportional to the wavelength).

There is a strong correlation between sunspots and the solar flux $F_{10.7}$ because probably most of the enhanced radiation comes from limited areas of the Sun where there are active sunspots. The activity depends on wavelength of radiated solar flux. For waves shorter than 3 cm, the intensity is steady. From 3 to 60 cm, often called decimeter range, the intensity shows occasional short-lived increases. These tend to last for a few minutes. The decimeter intensity also shows a slowly varying component that tends to exhibit a 27-day period associated with solar rotation (Reference 6) and rises from the vicinity of active sunspot regions. Large sporadic outbursts, lasting for minutes, occur often in association with the bigger solar flares. A millionfold increase in intensity within a few seconds has been observed. (This will be studied as a part of the sequence of the solar flux analysis by identifying the abrupt changes as one of seven Thom's "elementary catastrophes.") (See Section 5 for recommendations.)

It is necessary to study solar flux and accurately forecast it to perform accurate orbit determination for a spacecraft. The orbit lifetime is a function of atmospheric drag force; this force is a function of atmospheric density, which itself is a function of solar flux.

Section 2 is devoted mostly to graphical analysis of solar flux data. Section 3 describes the statistical techniques to compare different forecasting models by confidence interval methods. Section 4 introduces a linear, unbiased minimum-variance estimation and combines three important models into one. Section 5 is devoted to conclusions and recommendations for future investigations.

SECTION 2 - SOLAR FLUX $F_{10.7}$ PREDICTION

2.1 MATHEMATICAL PERSPECTIVES

For satellite orbit lifetime prediction, one has to evaluate the drag force that continually results in satellite orbit decay. By applying the fundamental principles of fluid mechanics, the drag force is written in the following form:

$$|\vec{F}| = \frac{1}{2} \rho \nu^2 C_d A \qquad (2\text{-}1)$$

where ρ is the atmospheric density, which is a complicated function of solar flux in different density models of the atmosphere. The velocity of the spacecraft is indicated by $\vec{\nu}$, and the other variables are properties of the spacecraft. These properties are drag coefficient C_d and scattering cross section A.

It is very clear from the above equation that, given the drag coefficient C_d and the scattering cross section A, one can easily calculate the drag force $|\vec{F}|$ if the density of the atmosphere is known. Since the atmospheric density is sensitive to solar activity, most of the density models are complicated functions of solar flux. The motivation for studying solar flux prediction models (other than solar astronomy) is the accurate satellite orbit lifetime prediction.

2.2 GRAPHICAL ANALYSIS OF DATA

The first part of this study compares Schatten solar flux forecasts with National Oceanic and Atmospheric Administration (NOAA) actual solar flux values. Schatten predictions are modified inconsistently, but at least once every 3 months. NOAA also forecasts short-term predictions that are modified consistently every week. Schatten's

latest values were distributed on September 1, 1990, which includes long-term predictions starting from September 1990 to September 2008. His next latest predictions were distributed on May 25, 1990, which includes predictions starting May 1990 to August 1990 and on to April 2012. Therefore his May 25 version, which includes May, June, July, and August 1990 predictions, is by far the best he could do. Thus this analysis was done on his best predictions (May, June, July, and August 1990).

As seen from the graphs in Figures 2-1 to 2-10, the 30-day mean of the actual (NOAA) values are always less than +2 sigma value of Schatten and in most cases are even smaller than Schatten (mean). They are closer to -2 sigma value or even smaller than that. This may mean that the mission analysis is being too conservative by using +2 sigma value consistently.

2.3 DESCRIPTION OF GRAPHS

Figures 2-1 to 2-10 present the actual solar flux values and different forecasts for the months of May, June, July, and August 1990. The forecasts are the best updates for those months. Figures 2-11 to 2-14 present the actual solar flux values and their different averages and different forecasts for a period of 2 years (October 15, 1988 to September 17, 1990). The actual data are daily values, and the long-term prediction models (Schatten and MSFC) are monthly values. Figures 2-15 and 2-16 are the confidence intervals for Schatten and MSFC forecasts, the nominal and the $+2\sigma$, respectively. Figures 2-17 to 2-19 are the actual solar flux values and their averages for three different timespans. The statistical analysis performed to get the confidence intervals is discussed in Section 3. It should be noted that all the units for the solar flux values are in units of

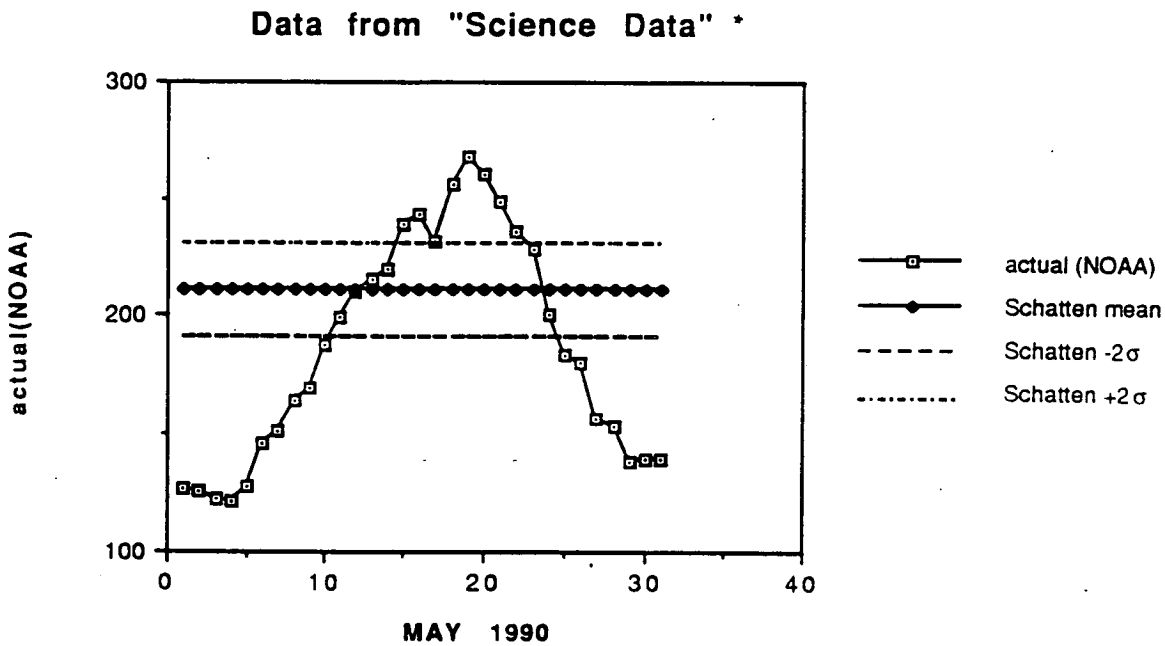

* Science data is a data file with its data printed by running a cricket graph on the Macintosh.

Figure 2-1. Plot of Solar Flux Values and Schatten Nominal, +2 Sigma, and -2 Sigma Predictions (May 1990)

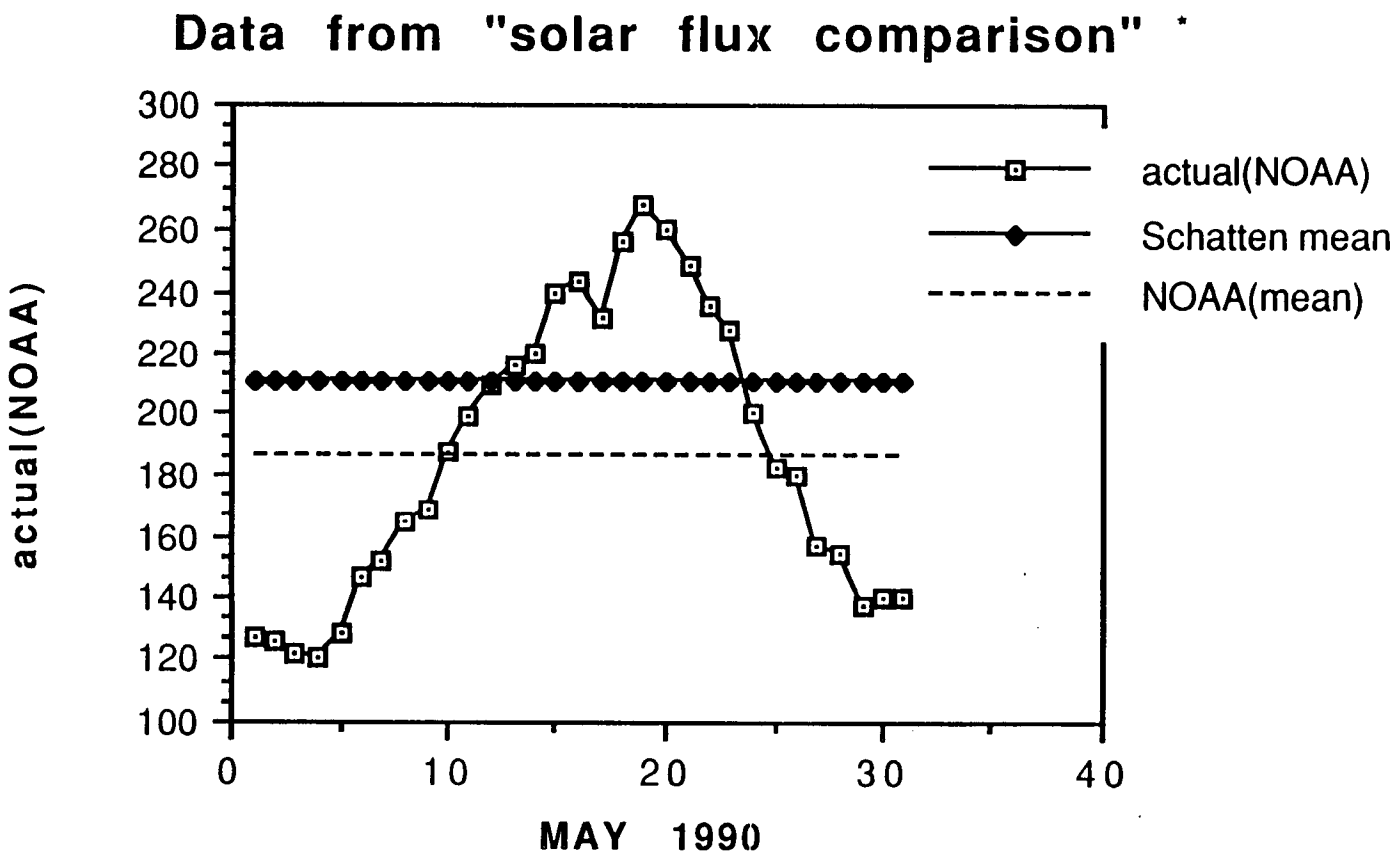

* Solar flux comparison is a data file with its data printed by running a cricket graph on the Macintosh.

Figure 2-2. Plot of Solar Flux Values, Schatten Nominal Prediction, and NOAA 27-Day Nominal Predictions (May 1990)

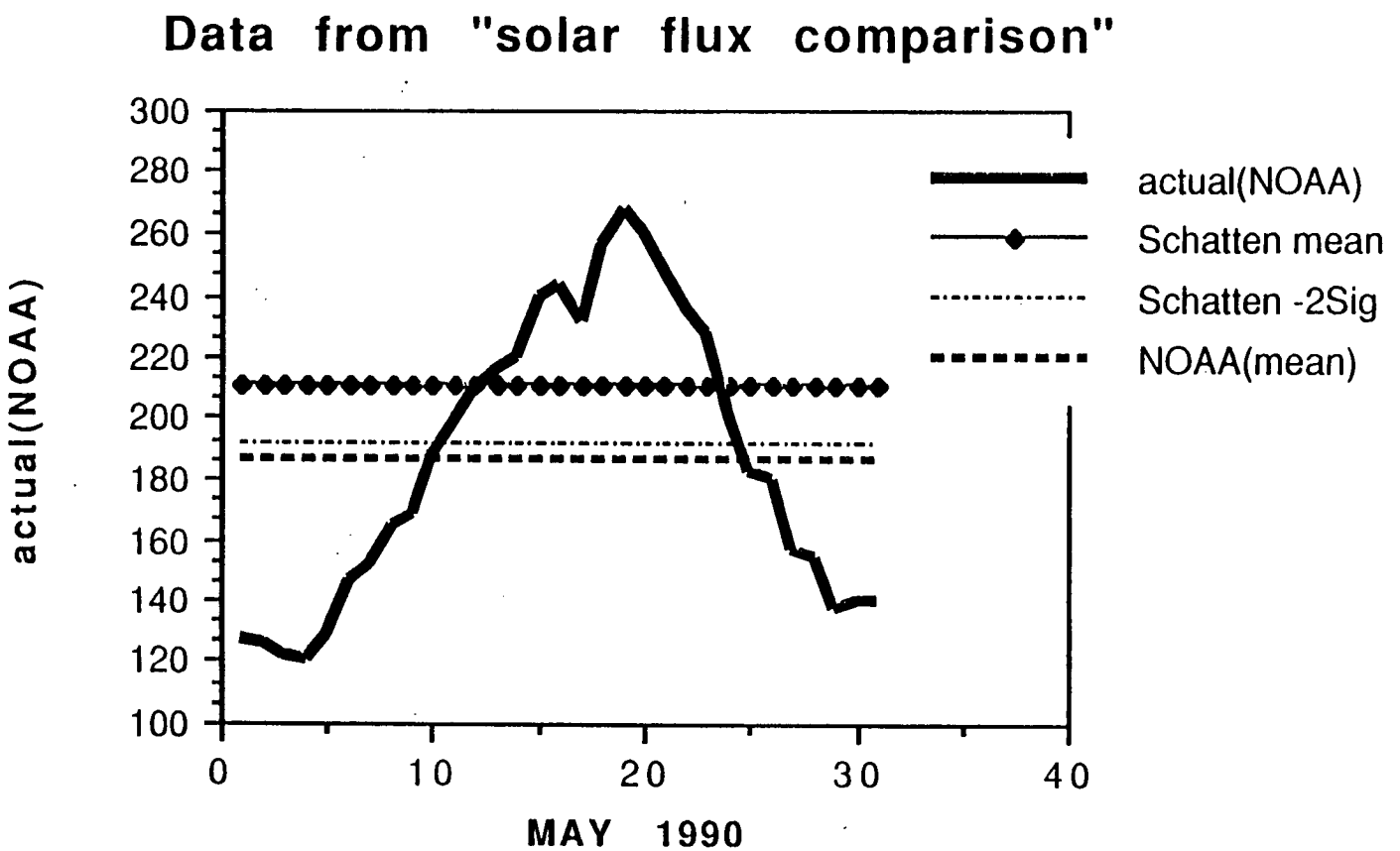

Figure 2-3. Plot of Solar Flux Values, Schatten Nominal and -2 Sigma Predictions, and NOAA 27-Day Nominal Predictions (May 1990)

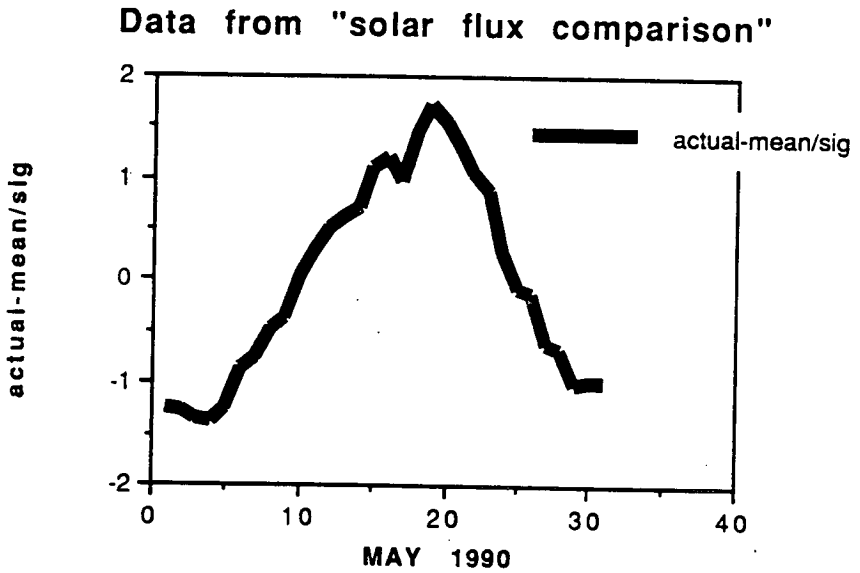

Figure 2-4. Plot of Solar Flux Values Minus the Mean Value Normalized by Standard Deviation (May 1990)

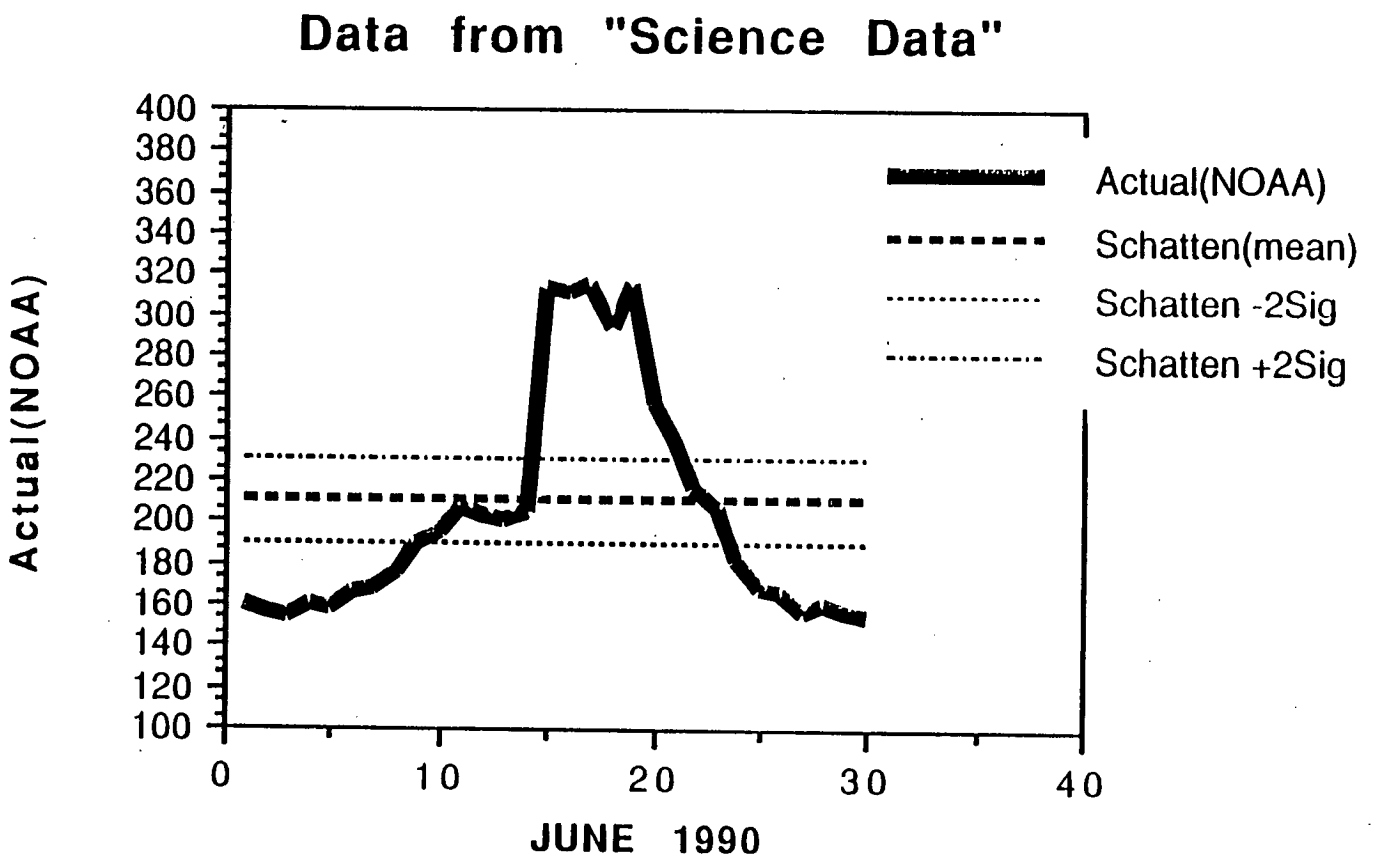

Figure 2-5. Plot of Solar Flux Values and the Schatten Nominal, +2 Sigma, and -2 Sigma Predictions (June 1990)

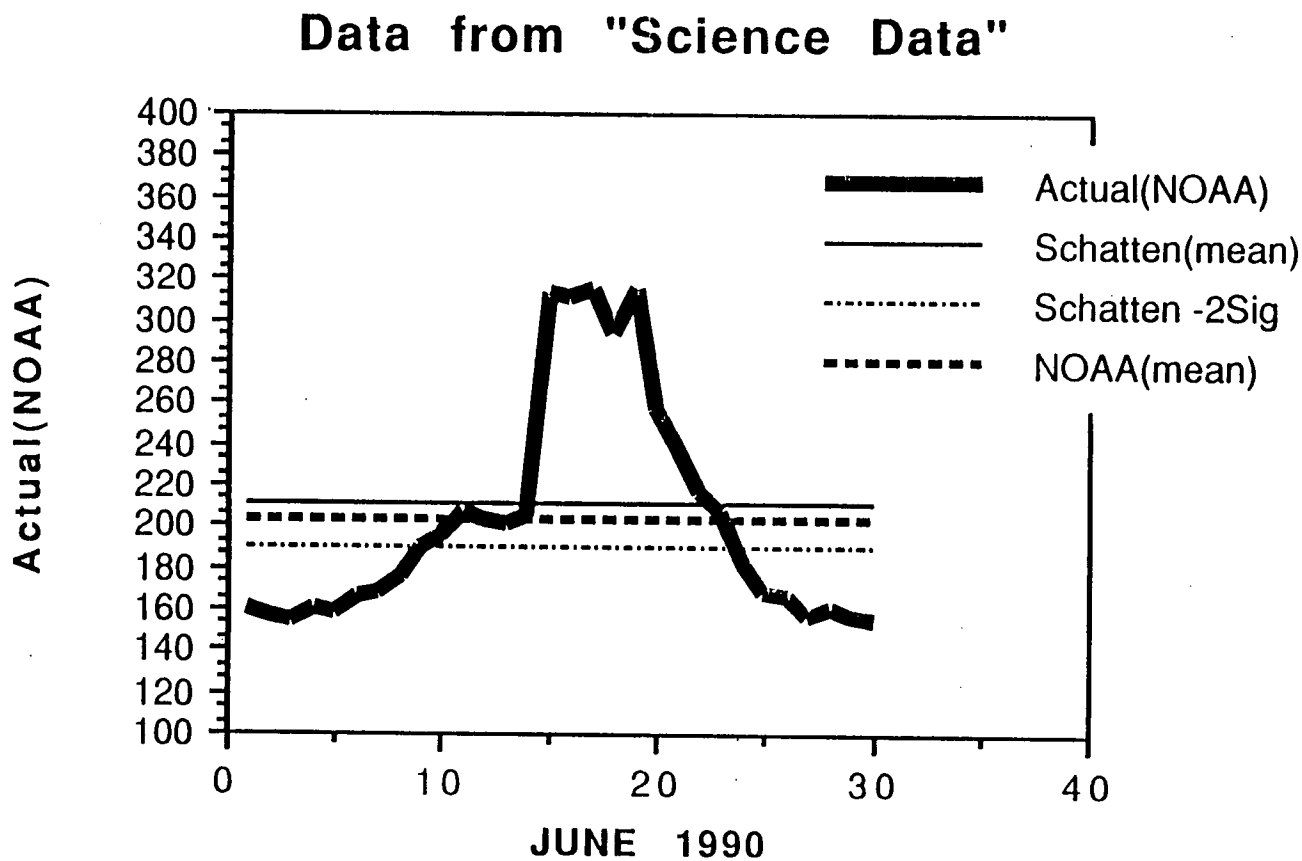

Figure 2-6. Plot of Solar Flux Values and the Schatten Nominal, -2 Sigma Predictions, and the NOAA 27-Day Nominal Predictions (June 1990)

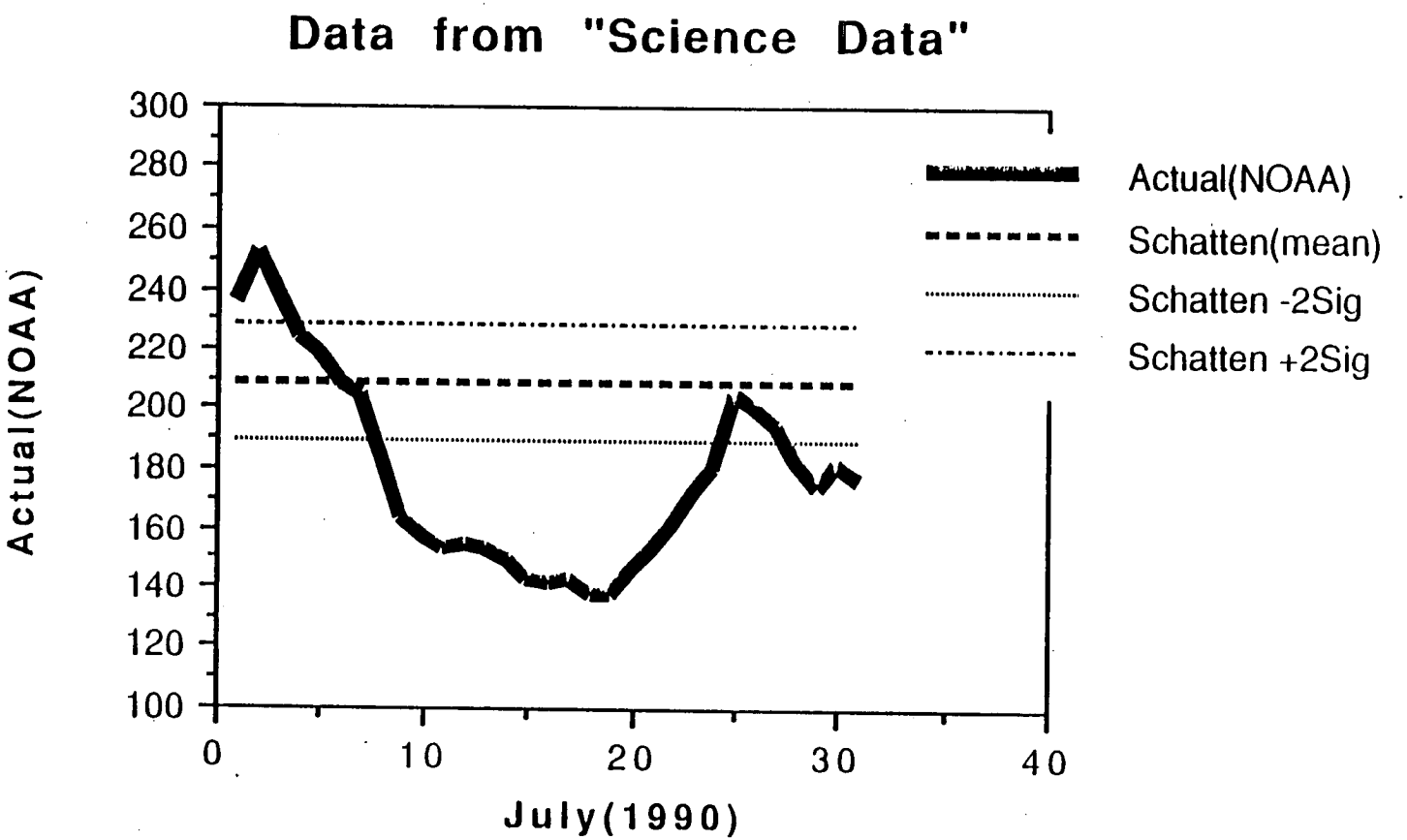

Figure 2-7. Plot of Solar Flux Values and the Schatten Nominal, +2 Sigma, and -2 Sigma Predictions (July 1990)

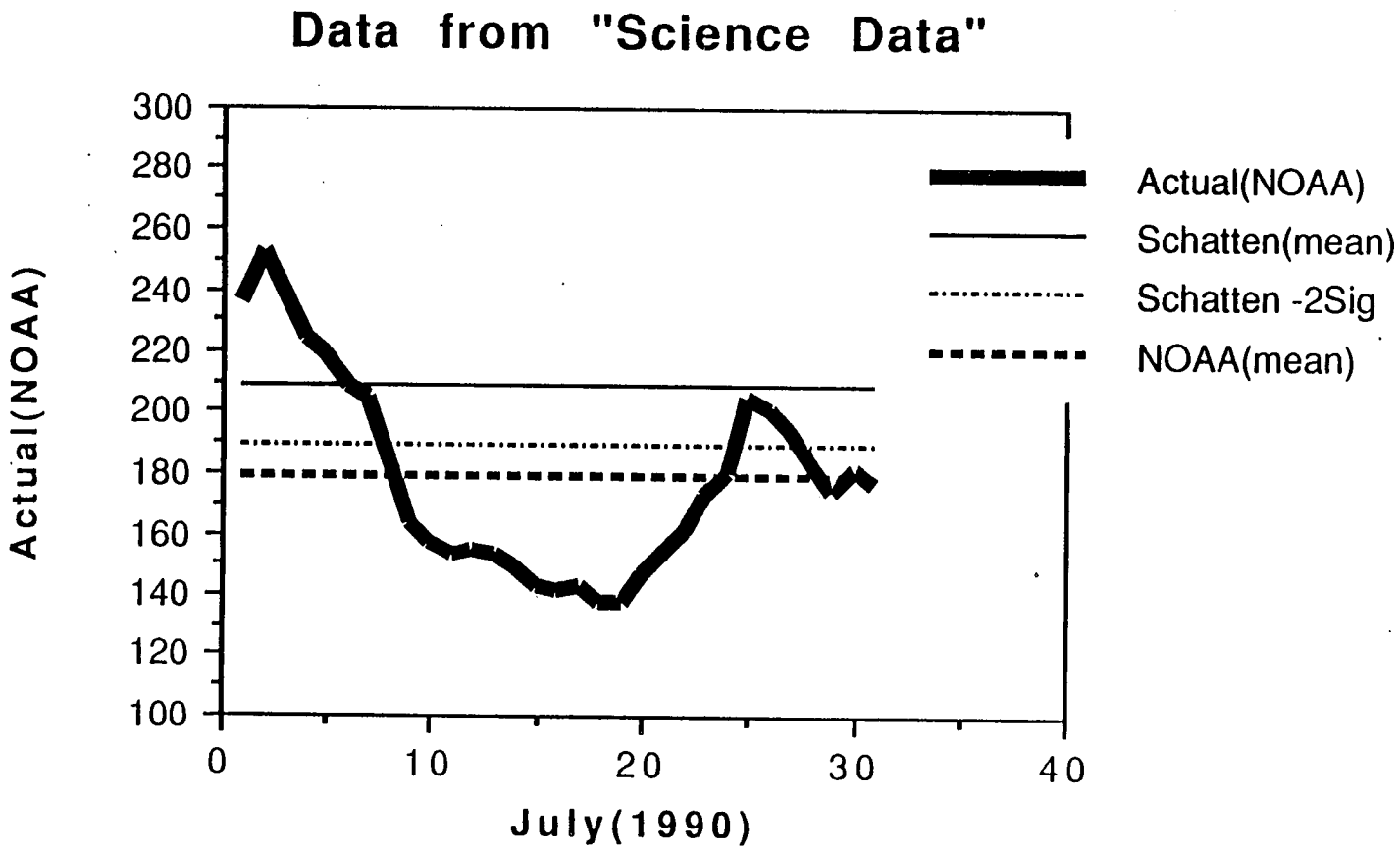

Figure 2-8. Plot of Solar Flux Values, the Schatten Nominal, -2 Sigma Predictions, and the NOAA 27-Day Nominal Predictions (July 1990)

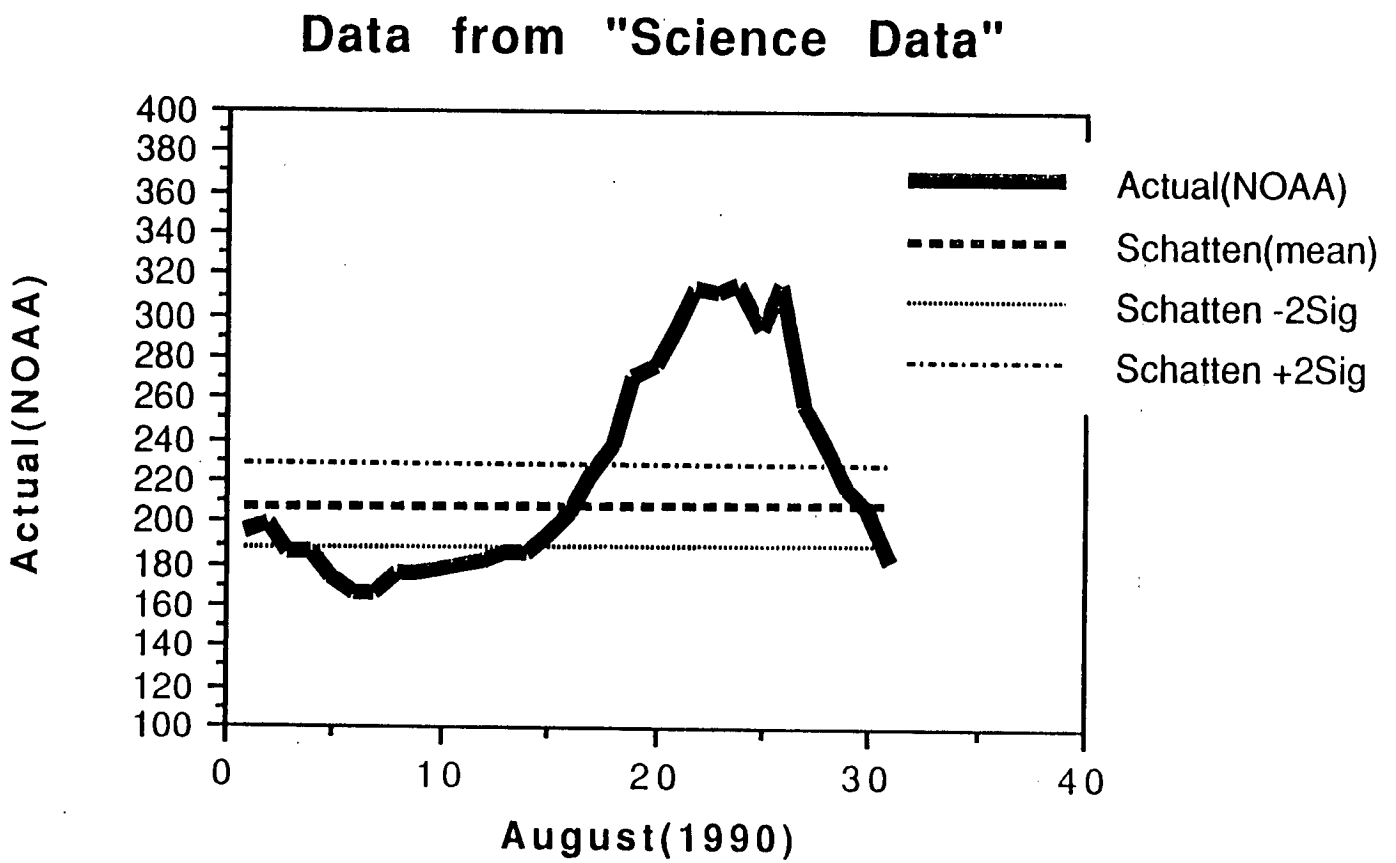

Figure 2-9. Plot of Solar Flux Values and the Schatten Nominal, -2 Sigma, and +2 Sigma Predictions (August 1990)

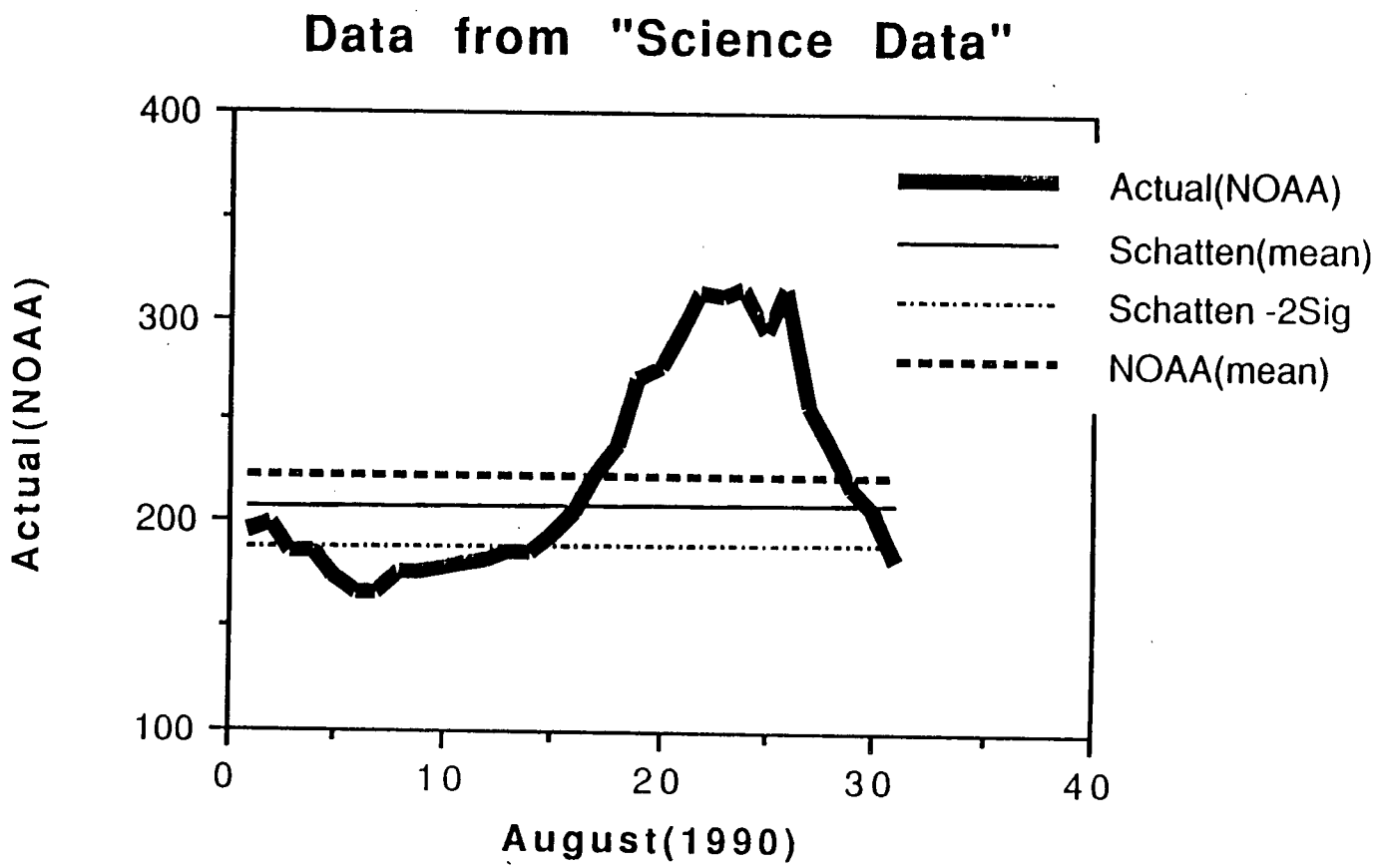

Figure 2-10. Plot of Solar Flux Values, the Schatten Nominal, -2 Sigma, and NOAA 27-Day Nominal Predictions (August 1990)

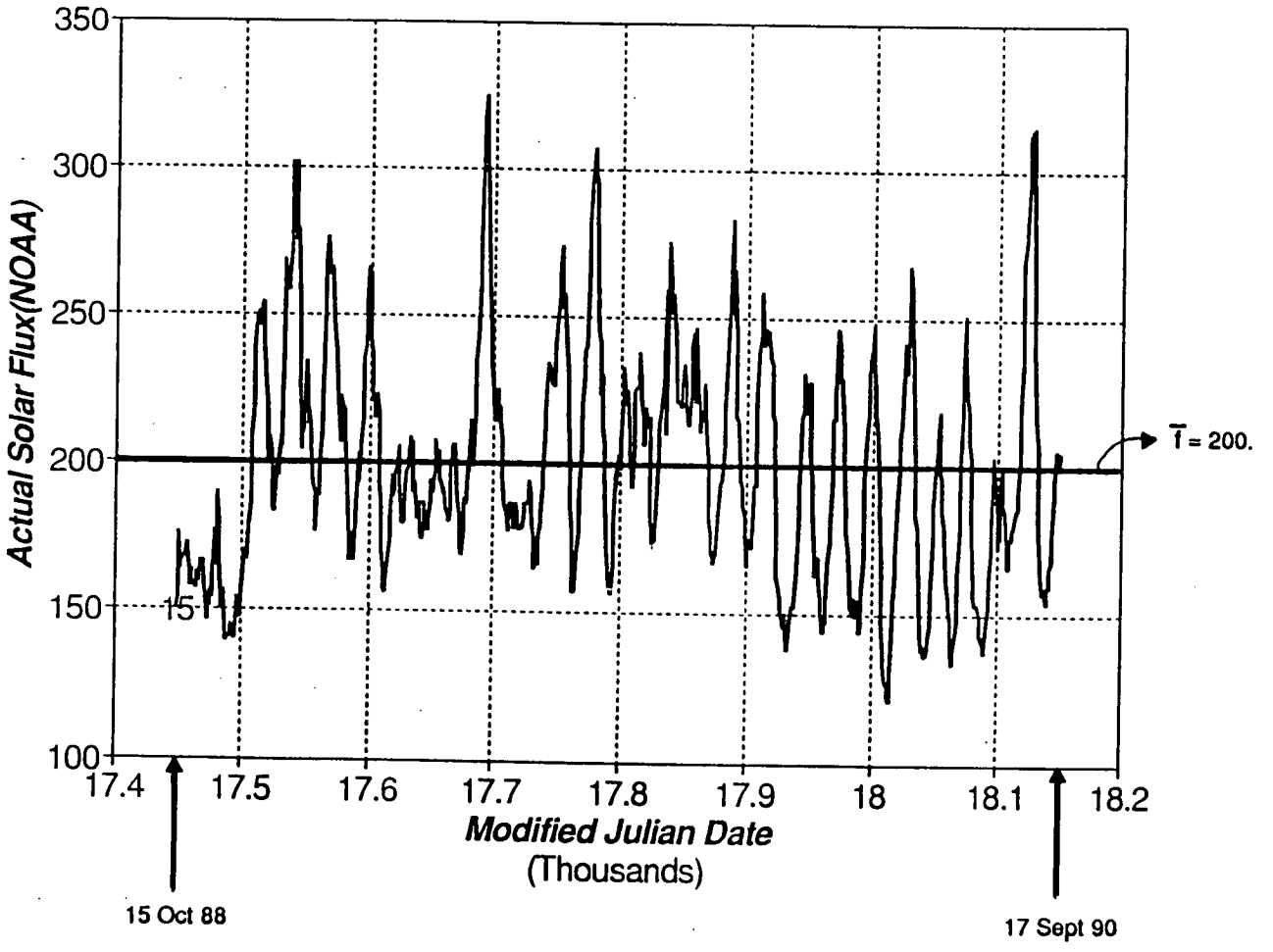

Figure 2-11. Plot of Actual NOAA Solar Flux Values for October 15, 1988, to September 17, 1990

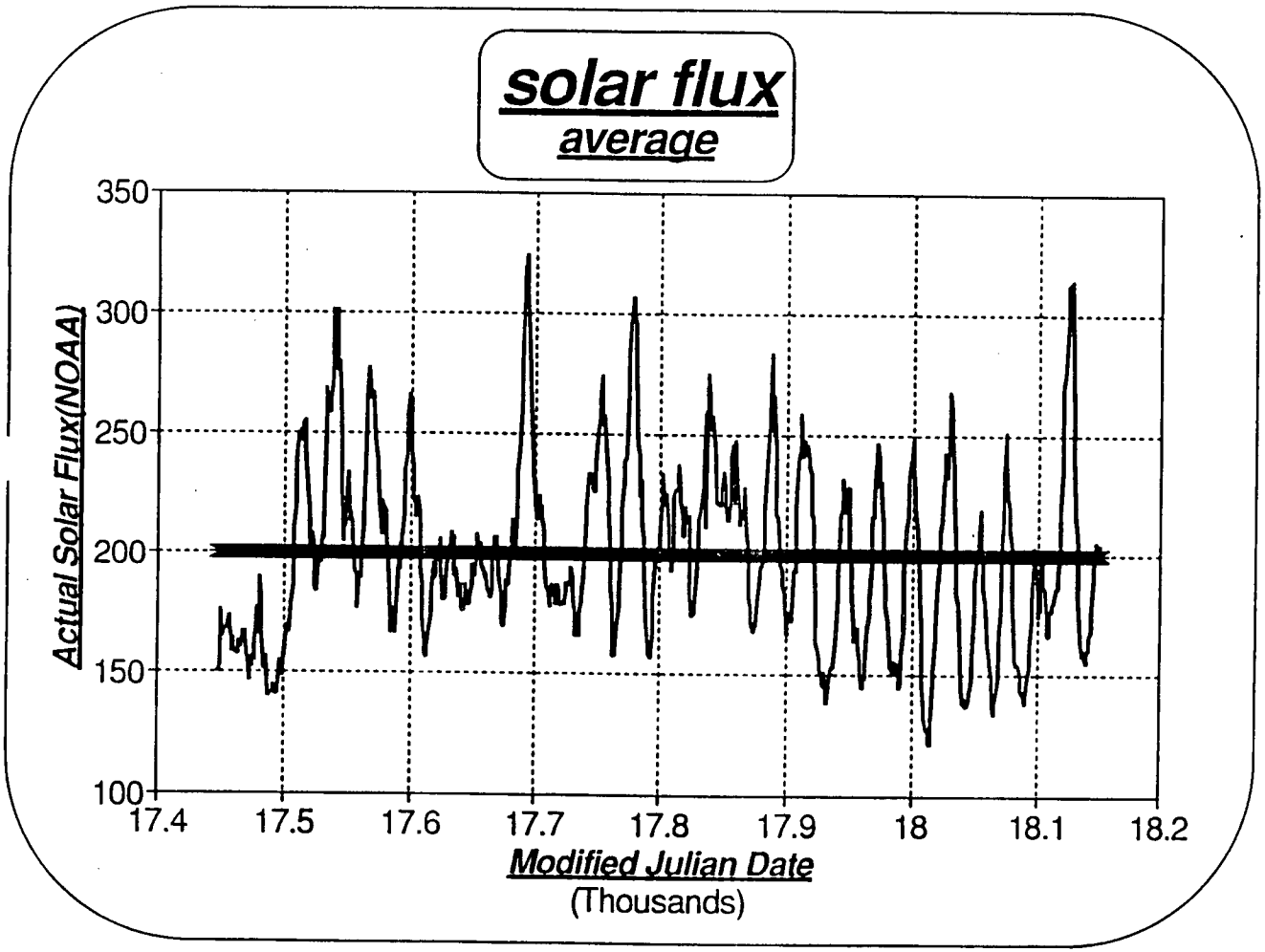

Figure 2-12. Plot of Actual Solar Flux Values and Mean Value

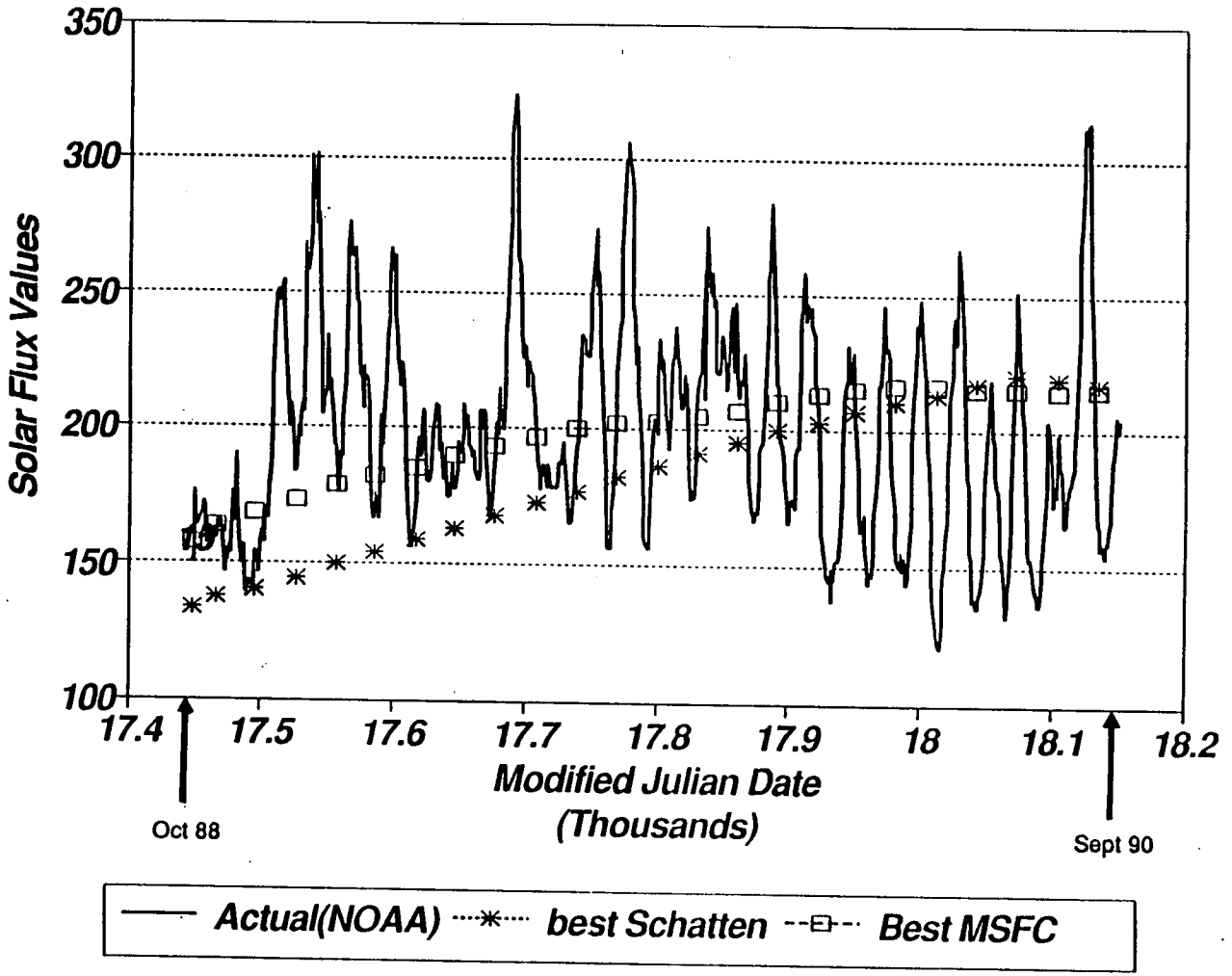

Figure 2-13. Plot of Solar Flux Values and the Nominal Best Schatten and MSFC Predictions

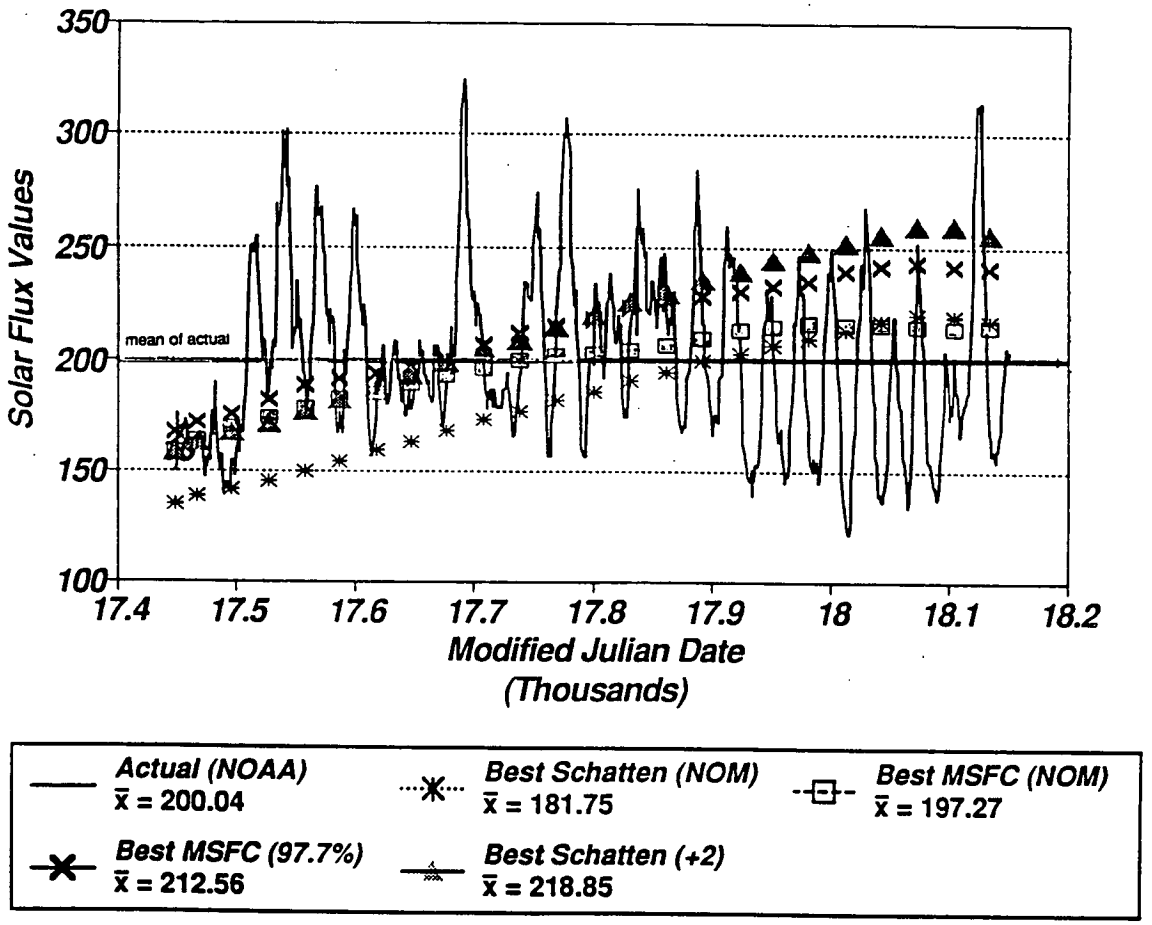

Figure 2-14. Plot of Solar Flux Values, the Schatten Nominal and +2 Sigma Predictions, and the MSFC Nominal and 97.7 Percent Predictions

6176

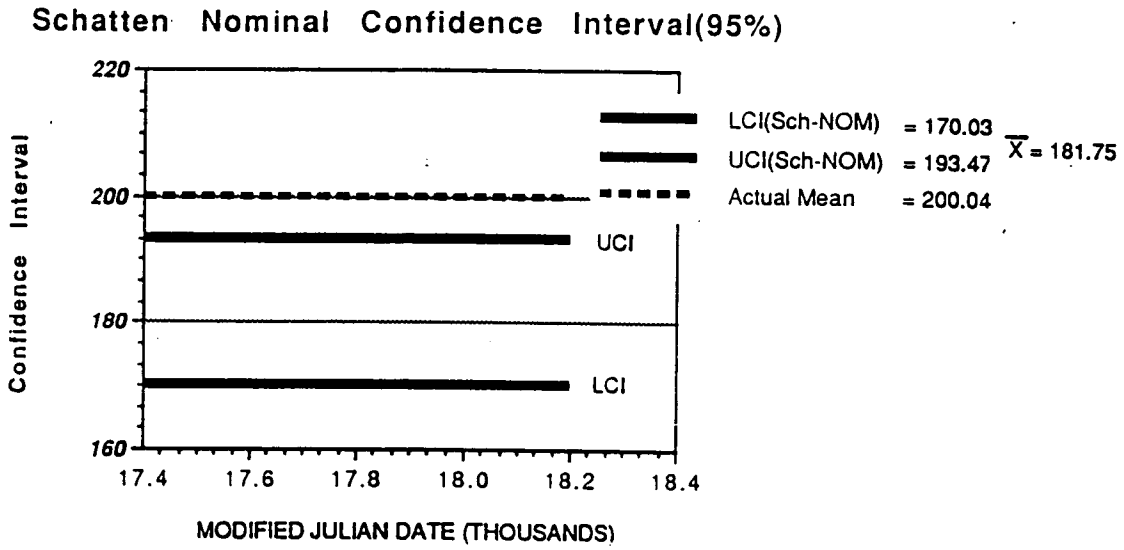

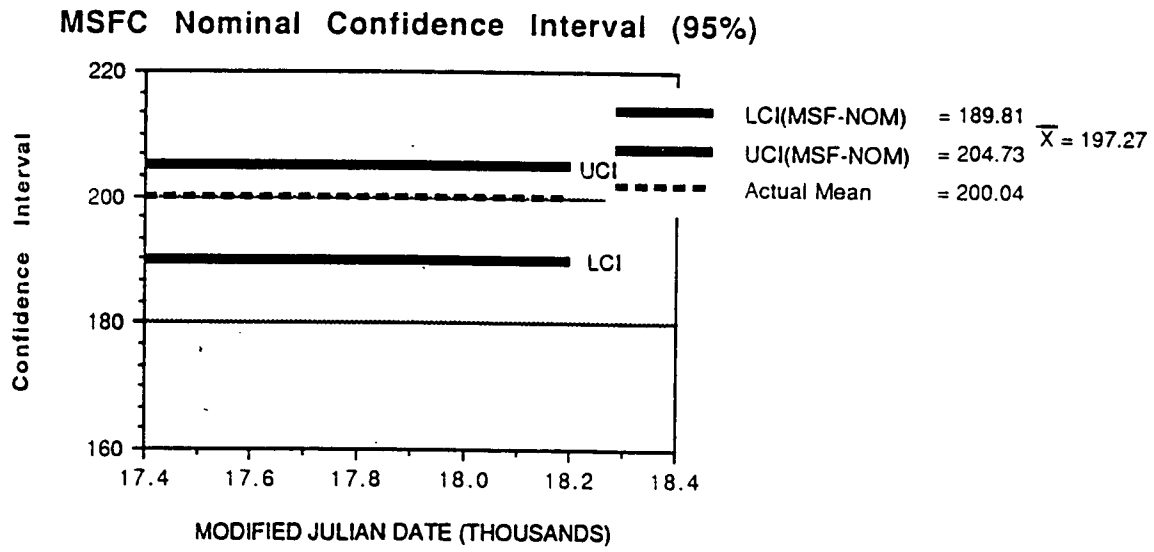

Figure 2-15. Plot of the Nominal Schatten and MSFC 95-Percent Predictions Confidence Interval and the Average of the Actual Solar Flux Values

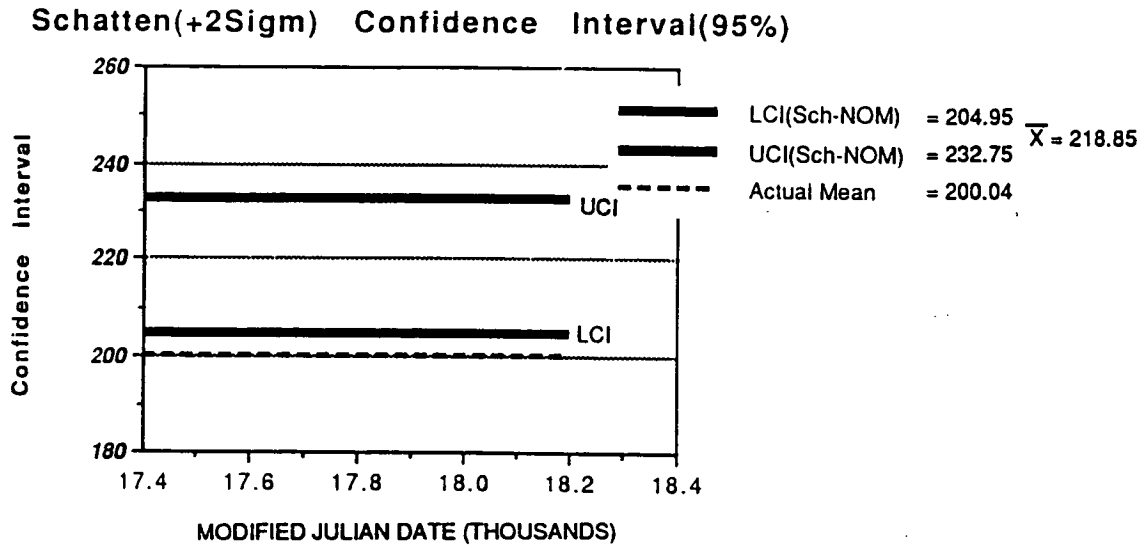

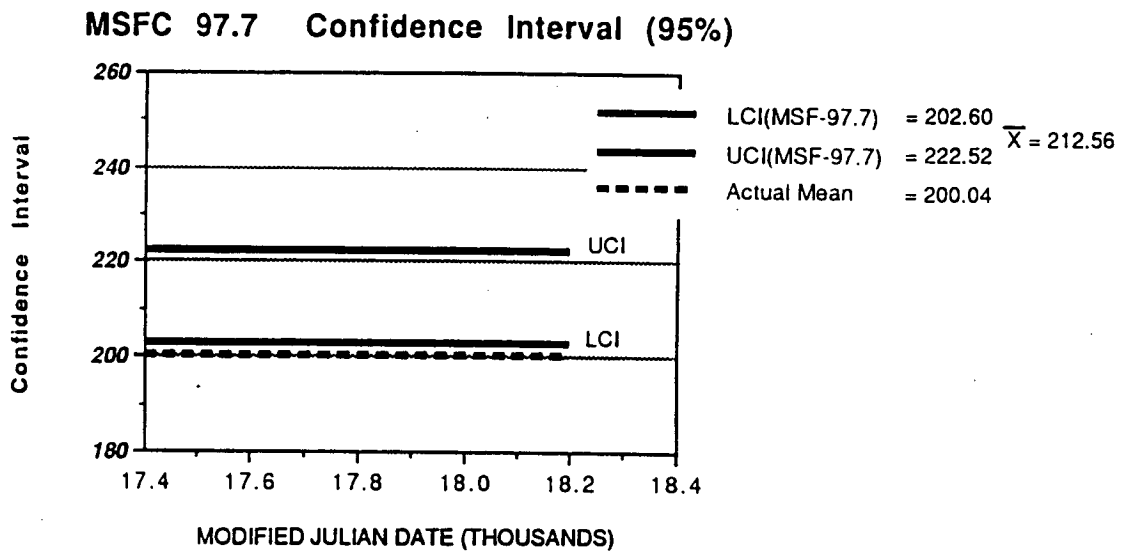

Figure 2-16. Plot of the Schatten +2 Sigma and MSFC 97.7-Percent Predictions Confidence Interval and the Average of the Actual Solar Flux Values

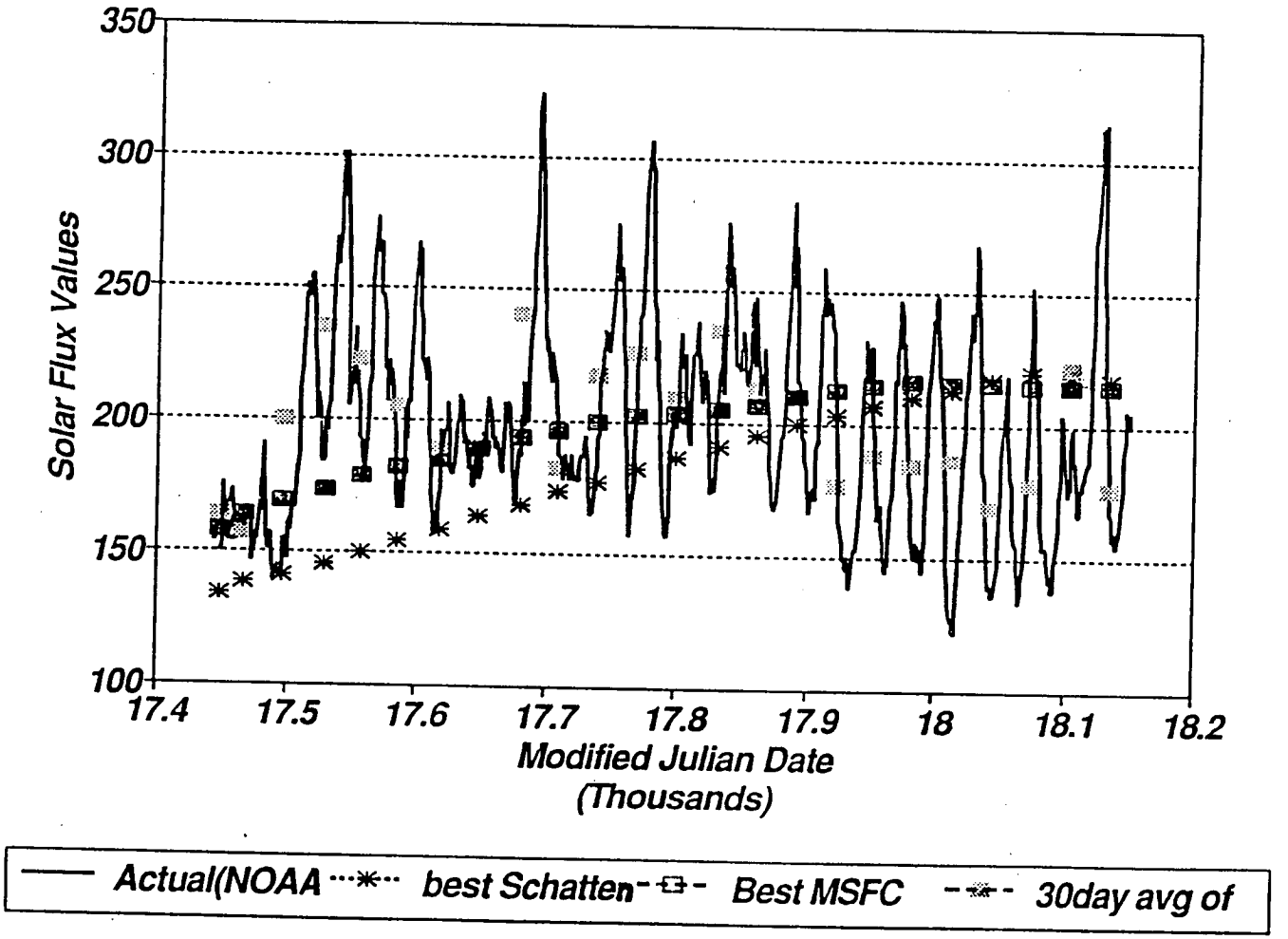

Figure 2-17. Plot of Actual Solar Flux Values From October 15, 1988, to September 17, 1990, and the Best Nominal Schatten and MSFC Prediction With the 30-Day Partitioned Average of Actual Solar Flux Values

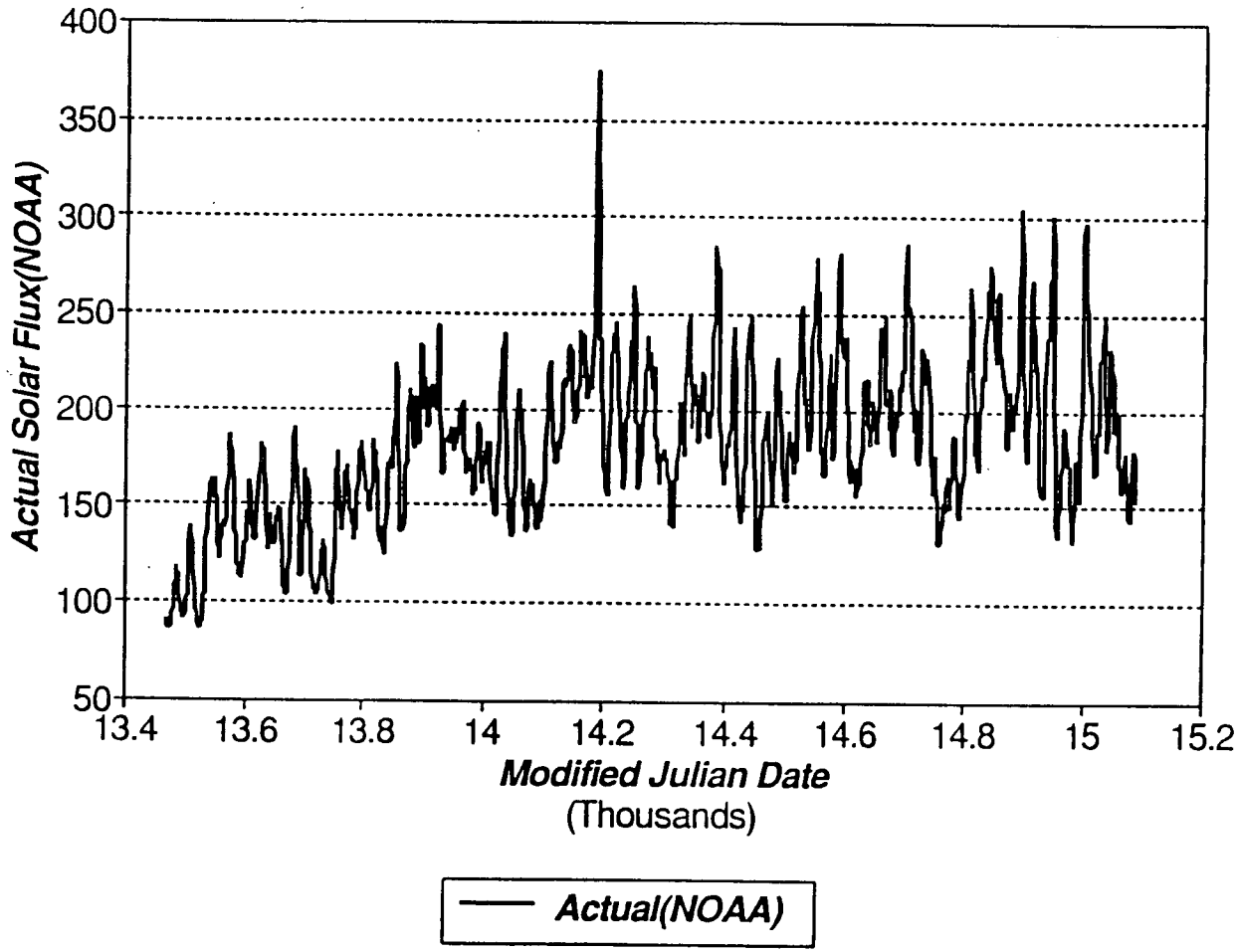

Figure 2-18. Plot of the Actual Solar Flux Values for a Different Timespan (MJD 13400 to 15200)

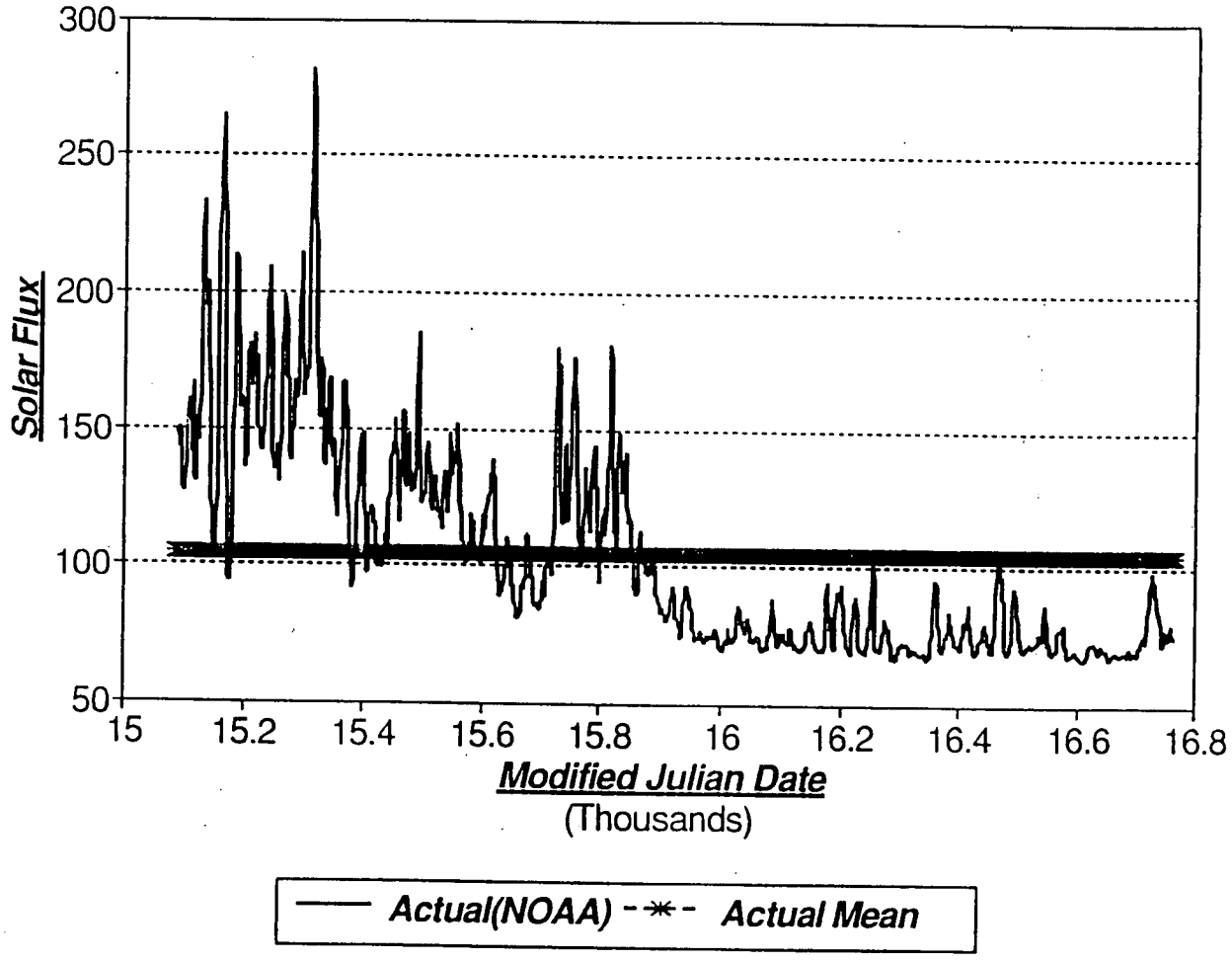

Figure 2-19. Plot of the Actual Solar Flux Values and Its Average for a Different Timespan (MJD 15000 to 16800)

watt/m^2/Hz x 10^{-22} for the range λ = 10.7 cm wavelength, and the horizontal axis is time in modified Julian date.

In order to compare forecast models of solar flux, one can compare the forecasts of solar flux ($F_{10.7}$) made for the timespan that the actual solar flux values are available. Every forecast will result in an interval (with a certain percentage of confidence). The actual population mean of data will fall within that confidence interval. This interval can be calculated for each forecast model. To compare forecast models, the question is whether the confidence interval encloses the population mean of the actual solar flux values or not. If it does, 95.5 percent of the time the predicted value is within the confidence interval; thus, it is a good forecast. The mathematical analysis of this procedure is presented in the next sections.

SECTION 3 - STATISTICAL ANALYSIS

3.1 CHECK OF A HYPOTHESIS

Sample values are often used as estimators for parameters of random variables. However, these procedures result only in point estimates for a parameter of interest; no indication is provided about how closely a sample value estimates the parameter. A more meaningful procedure for estimating parameters of random variables involves the estimation of an interval, as opposed to a single point value, which will include the parameter being estimated with a known degree of uncertainty. For example, consider the case where the sample mean $\bar{x}$ computed from N independent observations of a random variable x is being used as an estimator for the mean value μ_x. It is usually more desirable to estimate μ in terms of some interval d, such as $\bar{x} \pm d$, where there is a specified uncertainty that μ_x falls within that interval. Such intervals can be established if the sampling distribution of the estimator in question is known (Reference 7).

It can be shown that probability statements can be made concerning the value of a sample mean $\bar{x}$ as follows.

$$\text{prob}\left[z_{1-(\alpha/2)} < \frac{(\bar{x} - \mu_x)\sqrt{N}}{\sigma_x} \leq z_{\alpha/2}\right] = 1 - \alpha \qquad (3\text{-}1)$$

$$\text{prob}\left[\bar{x} > \left(\frac{\sigma_x z_\alpha}{\sqrt{N}} + \mu_x\right)\right] = \alpha \qquad (3\text{-}2)$$

where $\bar{x}$ = sample mean, μ_x = population mean, N = number of observations, σ_x = sample standard deviation, d = uncertainty length, α = probability measure, and z_α = desired percentage of confidence.

As the sample size N becomes large, the sampling distribution of the sample mean $\bar{x}$ approaches a normal distribution regardless of the distribution of the original variable x.

For a sample, the probability statement would be either 1 or 0, i.e.,

$$\text{prob}\left[z_{1-(\alpha/2)} < \frac{(\bar{x} - \mu_x)\ \sqrt{N}}{\sigma_x} \leq z_{\alpha/2}\right] = \begin{cases} 0 \\ 1 \end{cases} \qquad (3\text{-}3)$$

As the value α becomes small (as the interval between $z_{1-(\alpha/2)}$ and $z_{\alpha/2}$ becomes wide), the probability is more likely to be unity rather than zero. In slightly different terms, if many different samples were repeatedly collected and a value $\bar{x}$ were computed for each sample, one would expect

$$\text{prob}\ [\qquad] = \begin{cases} 0 \\ 1 \end{cases} \qquad (3\text{-}4)$$

to fall within the noted interval for about $1-\alpha$ of the samples. In this context a statement can be made about an interval within which one would expect to find the quantity

$$\frac{(\bar{x} - \mu_x)\ \sqrt{N}}{\sigma_x} \qquad (3\text{-}5)$$

with a small degree of uncertainty. Such a statement is called a confidence statement. The interval associated with the confidence statement is called a confidence interval.

For the case of the mean value estimate, a confidence interval can be established for the mean value μ_x based upon the sample value $\bar{x}$ by rearranging terms in the previous equation as follows:

$$\left[\bar{x} - \frac{\sigma_x \, z_{\alpha/2}}{\sqrt{N}} \leq \mu_x < \bar{x} + \frac{\sigma_x \, z_{\alpha/2}}{\sqrt{N}}\right] \qquad (3\text{-}6)$$

3.2 CHI-SQUARE DISTRIBUTION

For variance σ_x^2 based on the sample variance s^2 for a sample size of N = 31, one would use chi-square distribution χ^2

$$\left[\frac{n\ s^2}{x^2_{n;\alpha/2}} < \sigma_x^2 < \frac{n\ s^2}{x^2_{n;1-\alpha/2}}\right] \qquad n = N - 1 \qquad (3\text{-}7)$$

$$\left[\frac{30s^2}{x^2_{30;\alpha/2}} < \sigma_x^2 < \frac{30s^2}{x^2_{n;1-\alpha/2}}\right] \qquad n = 31 - 1 = 30 \qquad (3\text{-}8)$$

From a standard statistical table called, "Percentage Points of Chi-Square Distribution" (Reference 8) the value of $x^2_{n;\alpha/2}$ given α can be found.

For the value of $\alpha = 0.10$, $1 - \alpha/2 = 0.95$, and $\alpha/2 = 0.05$, $\chi^2_{30;\alpha/2} = 43.77$ and $\chi^2_{30;1-\alpha/2} = 18.49$.

So the interval reduces to

$$[0.6854s^2 \leq \sigma_x^2 < 1.622s^2] \qquad (3\text{-}9)$$

Calculate the sample mean $\bar{x}$ and the sample variance s^2 to find both intervals.

SECTION 4 - LINEAR, UNBIASED MINIMUM-VARIANCE ESTIMATION (LUMVE)

Schatten predictions are now adopted by GSFC because they apparently did a good job at some periods of time. But the conclusion from the data for the past 2 years is that MSFC predictions were closer to the actual solar flux values. This conclusion shows that it is not possible to compare the accuracy of two forecasting models (which use stochastic methods) when they try to model a time series that is inherently chaotic (existence of a structure in data). Therefore the best method is to combine all the models into one. This method is investigated in this section under linear, unbiased minimum-variance estimation (LUMVE). In this method, the three solar forecasting models--NOAA, MSFC, and Schatten predictions--are combined into one that minimizes the variance.

4.1 MATHEMATICAL FORMULATION

The LUMVE ensures that the variance of the combined solar flux predictions is the smallest that can be achieved for any linear, unbiased combination of the individual predictions. This method was used because it was demonstrated that MSFC predictions were closer to the actual solar flux than Schatten's for the past 2 years.

Solar flux is an inherently unpredictable phenomenon, and stochastic methods used by Schatten, MSFC, and NOAA cannot produce good predictions. Therefore, the dead-end approach before an analytic (not stochastic) nonlinear, chaotic approach is the linear, unbiased minimum-variance approach (References 9 and 10).

Let

σ_n = standard deviation of NOAA prediction
σ_m = standard deviation of MSFC prediction
σ_s = standard deviation of Schatten prediction

Consider a linear combination of the three flux predictions. Using normalized coefficients

$$\hat{f} = \frac{b_n f_n + b_m f_m + b_s f_s}{b_n + b_m + b_s} \tag{4-1}$$

where b_n, b_m, and b_s are coefficients for NOAA, MSFC, and Schatten forecast of solar flux f_n, f_m, and f_s, respectively.

Define

$$a_n = \frac{b_n}{b_n + b_m + b_s} \tag{4-2}$$

$$a_m = \frac{b_m}{b_n + b_m + b_s} \tag{4-3}$$

$$a_s = \frac{b_s}{b_n + b_m + b_s} \tag{4-4}$$

thus

$$\hat{f} = a_n f_n + a_m f_m + a_s f_s \tag{4-5}$$

Now the problem is to select values of a_n, a_m, and a_s that will yield the best $\hat{f}$ (the closest value to the mean of the actual data).

The variance of $\hat{f}$ is

$$V(\hat{f}) = a_n^2\sigma_n^2 + a_m^2\sigma_m^2 + a_s^2\sigma_s^2 + \underbrace{\text{covariance terms}}_{0 \text{ for independent predictions}} \tag{4-6}$$

By imposing $E(\hat{f}) = f$ (where f is the desired actual mean), and forcing the parameters

$$E(\hat{f}) = E(f_n) = E(f_m) = E(f_s) = f \tag{4-7}$$

which is a renormalization technique. Then,

$$E(\hat{f}) = a_n E(f_n) + a_m E(f_m) + a_s E(f_s) \tag{4-8}$$

and

$$f = a_n f + a_m f + a_s f \tag{4-9}$$

$$1 = a_n + a_m + a_s \tag{4-10}$$

Equation (4-6) then becomes

$$V(\hat{f}) = a_n^2\ \sigma_n^2 + a_m^2\ \sigma_m^2 + \left(1 - a_n - a_m\right)^2\ \sigma_s^2 \tag{4-11}$$

or

$$\begin{aligned} V(\hat{f}) = {} & a_n^2\ \left(\sigma_n^2 + \sigma_s^2\right) + a_m^2\ \left(\sigma_m^2 + \sigma_s^2\right) - 2a_n\ \sigma_s^2 - 2a_m\ \sigma_s^2 \\ & + 2a_n\ a_m\ \sigma_s^2 + \sigma_s^2 \end{aligned} \tag{4-12}$$

If the variance $V(\hat{f})$ is minimized (the ideal case), that is

$$\frac{\partial V(\hat{f})}{\partial a_n} = 0 \tag{4-13}$$

then $a_n\left(\sigma_n^2 + \sigma_s^2\right) + a_m\ \sigma_s^2 = \sigma_s^2$, and

$$\frac{\partial V(\hat{f})}{\partial a_m} = 0 \tag{4-14}$$

then $a_n\left(\sigma_s\right)^2 + a_m\left(\sigma_m^2 + \sigma_s^2\right) = \sigma_s^2$; therefore

$$a_n = \frac{\sigma_m^2\ \sigma_s^2}{\sigma_n^2\ \sigma_m^2 + \sigma_n^2\ \sigma_s^2 + \sigma_m^2\ \sigma_s^2} \tag{4-15}$$

$$a_m = \frac{\sigma_n^2\ \sigma_s^2}{\sigma_n^2\ \sigma_m^2 + \sigma_n^2\ \sigma_s^2 + \sigma_m^2\ \sigma_s^2} \tag{4-16}$$

$$a_s = \frac{\sigma_n^2\ \sigma_m^2}{\sigma_n^2\ \sigma_m^2 + \sigma_n^2\ \sigma_s^2 + \sigma_m^2\ \sigma_s^2} \tag{4-17}$$

By dividing by $\sigma_n^2\ \sigma_m^2\ \sigma_s^2$

$$a_n = \frac{1/\sigma_n^2}{1/\sigma_n^2 + 1/\sigma_m^2 + 1/\sigma_s^2} = \frac{\omega_n}{\omega_n + \omega_m + \omega_s} \tag{4-18}$$

$$a_m = \frac{1/\sigma_m^2}{1/\sigma_n^2 + 1/\sigma_m^2 + 1/\sigma_s^2} = \frac{\omega_m}{\omega_n + \omega_m + \omega_s} \tag{4-19}$$

and

$$a_s = \frac{1/\sigma_s^2}{1/\sigma_n^2 + 1/\sigma_m^2 + 1/\sigma_s^2} = \frac{\omega_s}{\omega_n + \omega_m + \omega_s} \tag{4-20}$$

where

$$\omega_n = \frac{1}{\sigma_n^2}$$

$$\omega_m = \frac{1}{\sigma_m^2}$$

$$\omega_s = \frac{1}{\sigma_s^2} \qquad (4\text{-}21)$$

$$f = \frac{\omega_n f_n + \omega_m f_m + \omega_s f_s}{\omega_n + \omega_m + \omega_s}$$

This approach requires only the ratios of the coefficients (a_n, a_m, a_s) and not the actual parameters. See Figure 4-1 for calculations of these parameters. The variances are calculated on the PC (IBM AT compatible) using the Quattro Pro program.

Can the same coefficients be used in the future or do these coefficients vary with time? If they vary in time are the variations predictable or not? Figures 4-1 through 4-10 show that these coefficients evolve in time in a predictable fashion. The reason they are predictable is that all the variations are already in the flux values and their adjustment coefficients a_n, a_m, a_s do not vary violently and are predictable (Figures 4-1 through 4-10).

4.2 GRAPHICAL ANALYSIS OF DATA

The calculations of the required parameters in LUMVE presented in the previous section is performed here. The intermediate coefficients--a_n, a_m, and a_s--are calculated from Equations (4-15) through (4-21) and presented in Figure 4-1.

Science Data

Thu, Oct 18, 1990 7:31 AM

	NOAA m	MSFC m	Schatten m	NOAA sn	MSFC sn	Schatten sn	sig n**2	sig m**2	sig s**2	sig nm**2	sig ns**2	sig ms**2	Eff	An	Am	As	An*Fn	Am*Fm	As*Fs	Our Flux
1	188.5217381	109.7000000	100.0000000	0.084044697	0.00000000	0.00000000	65.35177666	0.00000000	0.00000000	0.000	0.000	0.000	0.000							
2	188.5217381	112.6600000	102.0000000	0.084044697	4.03050865	2.82842713	65.35177666	16.24500000	8.00000000	1061.640	622.614	129.960	1714.414	0.07580433	0.30495217	0.61824350	15.12461233	34.32236662	63.16283681	112.6098151
3	188.5217381	115.4333333	104.0000000	0.084044697	6.75607246	4.00000000	65.35177666	33.06333334	16.00000000	2160.748	1045.628	528.013	3735.385	0.14162200	0.27892489	0.57945311	28.25666832	32.31268267	60.15912363	120.7284541
4	188.5217381	118.1500000	106.7500000	0.084044697	7.18076133	4.78713654	65.35177666	51.66333334	22.91666667	3389.756	1497.646	1181.660	6049.060	0.19534600	0.24758308	0.65707082	38.87677394	29.25194036	58.91026010	127.1379844
5	188.5217381	120.6800000	107.8000000	0.084044697	8.40606140	5.65462019	65.35177666	70.67700000	34.30000000	4618.868	2241.546	2424.221	9284.655	0.26109976	0.24142696	0.69747328	52.09507751	29.13540586	63.62812491	134.7568509
6	188.5217381	123.0566667	109.8000000	0.084044697	9.62403473	7.00713922	65.35177666	90.71666666	49.10000001	5928.626	3206.772	4454.267	13681.685	0.32772143	0.23408348	0.43619600	65.38755053	29.05600710	47.76336174	142.2049191
7	188.5217381	125.4571429	111.4285714	0.084044697	10.75172190	8.18246348	65.35177666	115.69952381	66.05238096	7554.634	4376.457	7739.663	19669.766	0.38348041	0.22244594	0.38407364	78.50789654	27.90743230	42.79677747	149.2121061
8	188.5217381	127.0500000	113.2500000	0.084044697	12.18438055	9.18125361	65.35177666	145.60000013	83.82857143	9724.346	5454.861	12488.671	27697.788	0.45088661	0.19802591	0.35108720	89.95171949	25.33741455	38.76063558	155.0597691
9	188.5217381	128.6666667	115.1111111	0.084044697	13.65000000	10.22795733	65.35177666	181.22250000	104.61111114	12535.842	6636.522	20066.766	38438.229	0.50890216	0.17334320	0.31786463	101.61709264	22.63284411	36.58860008	160.7365361
10	188.5217381	133.3000000	117.0000000	0.084044697	15.66850191	11.34313502	65.35177666	246.22500007	128.66666671	16026.863	8408.686	31651.640	55985.780	0.56356506	0.15019158	0.26424336	112.44348050	20.02063761	33.49047318	165.9544911
11	188.5217381	136.0636364	118.9090909	0.084044697	17.45601740	12.48562810	65.35177666	304.71254556	155.09090908	19913.507	10167.748	47601.818	77603.171	0.61211306	0.13128006	0.25680687	122.12986590	17.66244107	30.61268676	170.5051967
12	188.5217381	138.8000000	120.7500000	0.084044697	19.18368487	13.60604550	65.35177666	366.66363644	182.30833362	23978.191	11918.273	66910.926	102868.389	0.66065036	0.11594018	0.23320946	129.85079590	16.09249623	28.16064454	174.1111334
13	188.5217381	141.4692308	122.6153846	0.084044697	20.71023039	14.67474106	65.35177666	428.91307417	212.42307697	28038.291	13882.226	91111.228	133023.743	0.69492456	0.10435801	0.21071548	136.65733545	14.76368863	25.63707872	177.2540021
14	188.5217381	144.1142857	124.5714286	0.084044697	22.22318384	15.80026429	65.35177666	493.66901106	240.64285163	32275.218	15314.964	123293.685	171883.767	0.71730790	0.09481858	0.18772351	143.11552044	13.67912400	23.38121448	180.1686591
15	188.5217381	146.4600000	126.5333333	0.084044697	23.57545546	17.01623874	65.35177666	555.50257168	269.56238088	36322.687	16922.763	160533.956	216179.408	0.74444629	0.08763268	0.16802103	148.63321036	12.83764288	21.26026053	182.6310222
16	188.5217381	149.0667500	128.6625000	0.084044697	24.73018986	18.33382676	65.35177666	611.66220150	336.12916663	39867.991	18968.638	205570.646	267606.275	0.76847324	0.08211656	0.14941010	153.32711748	12.24102739	19.20853627	184.7764811
17	188.5217381	151.4529412	130.8882353	0.084044697	25.88421616	19.61841872	65.35177666	659.99264726	384.88235307	43785.211	20152.746	257866.347	326808.304	0.78905581	0.07686530	0.13307909	157.43374691	11.65682167	17.49613310	186.5850114
18	188.5217381	153.7833333	132.6666667	0.084044697	26.90767141	20.97637686	65.35177666	728.33440813	439.95555555	47697.849	20754.703	320467.139	396819.873	0.80758844	0.07246306	0.11994050	161.13144962	11.14361109	15.91316791	188.1682278
19	188.5217381	156.0316789	134.7684737	0.084044697	27.99837201	22.36864786	65.35177666	783.90894720	501.17643862	51220.844	22752.706	392676.010	476858.461	0.82388368	0.06868434	0.10743197	164.38270765	10.71692526	14.46068674	188.5603311
20	188.5217381	158.2250000	136.8000000	0.084044697	28.88329576	23.74624624	65.35177666	836.67250012	563.88421049	54821.610	26850.636	473026.657	564699.404	0.83768122	0.06525741	0.09708137	167.13162291	10.32535442	13.25043926	190.7474161
21	188.5217381	160.3142857	138.8428180	0.084044697	29.80933219	25.15049838	65.35177666	882.69426561	632.84761908	58071.248	31338.112	562079.455	661488.925	0.84871463	0.06249252	0.08778884	169.63733942	10.01844423	12.20682968	191.7626132
22	188.5217381	162.2546466	141.1818182	0.084044697	30.48119994	26.60720722	65.35177666	929.15035478	702.63203460	60716.678	35818.253	657817.818	759434.740	0.85956705	0.05846213	0.07985021	171.60642336	9.81025584	11.28751666	192.6041951
23	188.5217381	164.1000000	143.3478261	0.084044697	31.06771187	27.90341888	65.35177666	965.20272705	778.60878077	63077.715	40882.847	751507.607	865468.268	0.86832485	0.05478239	0.07260276	173.24984475	9.64703093	10.44758503	193.3451009
24	188.5217381	165.6833333	145.8000000	0.084044697	31.61588300	29.25698168	65.35177666	999.56405707	855.01304333	65323.268	45935.440	855539.916	976790.844	0.87588108	0.05126404	0.06687688	174.75332588	9.49516037	9.73028459	193.9827701
25	188.5217381	167.0450000	147.8000000	0.084044697	32.10333057	30.64408889	65.35177666	1035.76676658	930.06000003	67688.200	51349.241	972847.140	1101708.662	0.88266178	0.05570386	0.06144037	176.14692047	9.33853888	9.07361410	194.5610734
26	188.5217381	168.3923077	149.8076923	0.084044697	32.76345431	31.92493608	65.35177666	1073.44393832	1019.20163868	70161.471	56606.633	1084055.714	1230813.818	0.88788007	0.05411593	0.05698801	177.36248273	9.18662212	8.83844000	195.0577541
27	188.5217381	171.0777778	151.9259259	0.084044697	33.29954185	33.18365237	65.35177666	1108.85948742	1101.14814798	72485.840	71961.990	1221018.671	1365446.501	0.89422658	0.05270217	0.05307124	178.41764478	9.01818968	8.60629737	195.4967111
28	188.5217381	172.6882857	154.0000000	0.084044697	33.77137007	34.36288612	65.35177666	1140.60543640	1180.81481608	74534.059	77166.348	1348725.718	1498420.123	0.89875687	0.05149963	0.04974180	179.32185263	8.89341755	7.66019002	195.8755601
29	188.5217381	174.1783103	156.0344828	0.084044697	34.11076156	35.47786294	65.35177666	1164.15812823	1258.67733916	76079.804	82258.603	1485299.456	1623436.063	0.90248024	0.05066209	0.04685767	180.08442600	8.82428660	7.31141245	196.2001271
30	188.5217381	175.5466667	158.0666667	0.084044697	34.35268115	36.68464190	65.35177666	1180.10464370	1330.16781879	77121.937	87516.999	1580356.168	1744897.084	0.90565088	0.05015309	0.04418603	180.68703906	8.80420801	6.98591858	196.4871651
31	188.5217381	176.8148290	160.0461161	0.084044697	34.50469914	37.85982629	65.35177666	1190.72538812	1418.26236555	77816.023	92665.968	1688741.020	1859263.011	0.90829883	0.04988002	0.04185316	181.22478297	8.81444638	6.69920498	196.7384341
32	188.5217381	177.9675000	161.9062500	0.084044697	34.58644848	38.48400000	65.35177666	1196.22241916	1481.01825600	78178.263	96787.177	1771627.241	1946589.801	0.91011848	0.04872141	0.04016011	181.68842186	8.84978888	6.50217340	196.9403847
33	188.5217381	179.1080909	163.6767676	0.084044697	34.64611598	38.07367264	65.35177666	1200.35335250	1528.75188358	78446.227	99776.952	1832641.764	2010862.932	0.91137080	0.04861847	0.03901073	181.83828644	8.88711992	6.38120936	197.1086151

Intermediate calculations of equation (4-15) through equation (4-21)

where

NOAA-m:	NOAA nominal prediction f_n (Solar Flux)	DEN:	$\sigma_n^2\sigma_m^2+\sigma_n^2\sigma_s^2+\sigma_m^2\sigma_s^2$
MSFC-m:	MSFC nominal prediction f_m (Solar Flux)	A_n:	a_n
Schatten-m:	Schatten nominal prediction f_s (Solar Flux)	A_m:	a_m
NOAA-sn:	σ_n	A_s:	a_s
MSFC-sn:	σ_m	$A_n * f_n$:	$a_n f_n$
Schatten:	σ_s	$A_m * f_m$:	$a_m f_m$
Sig-n **2:	σ_n^2	$A_s * f_s$:	$a_s f_s$
Sig-m **2:	σ_m^2	Our Flux:	$f = a_n f_a + a_m f_m + a_s f_s$
Sig-s **2:	σ_s^2		
Sig-nm **2:	$\sigma_n^2\sigma_m^2$		
Sig-ns **2:	$\sigma_n^2\sigma_s^2$		
Sig-ms **2:	$\sigma_m\sigma_s^2$		

Figure 4-1. Calculation of the Parameters Used in Linear, Unbiased Minimum-Variance Estimation (Running Procedure: Running Average of Data)

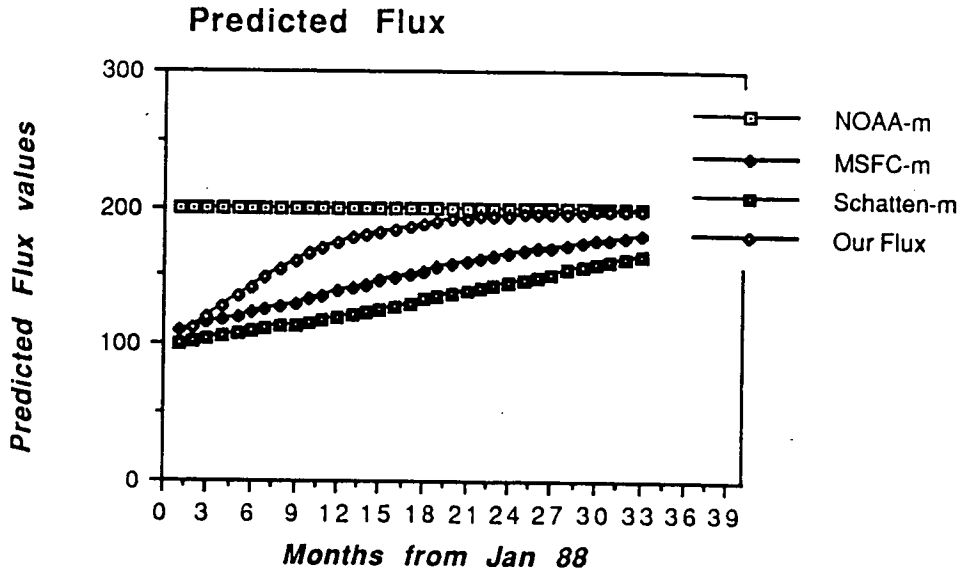

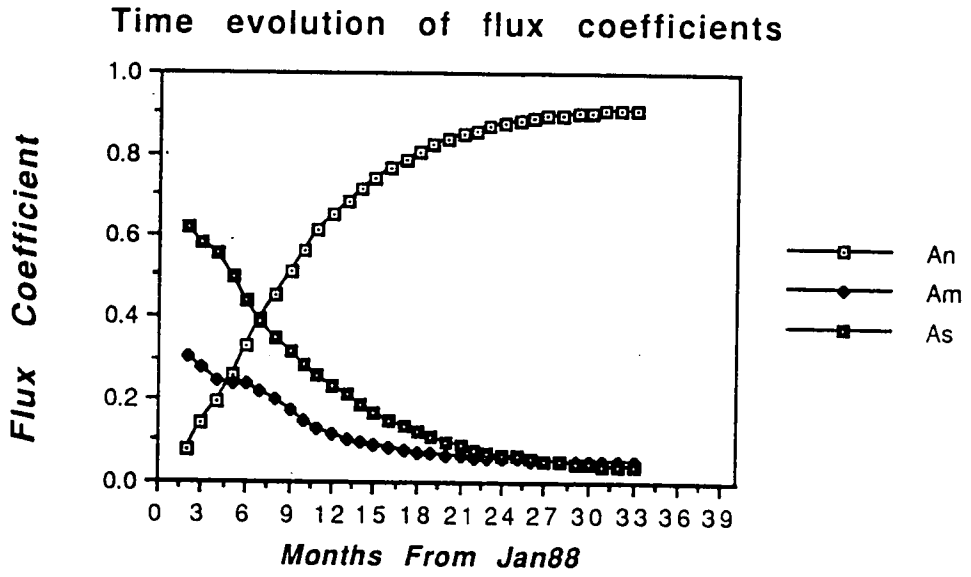

Figure 4-2. Predicted Flux by NOAA, MSFC, Schatten (Nominals) and the Result of Linear, Unbiased Minimum-Variance Estimation (Time Evolution of the Coefficients a_n, a_m, and a_s--Running Procedure)

6176

Partitioned

Fri, Oct 19, 1990 12:39 AM

	NOAA m	MSFC m	Schatten m	NOAA sn	MSFC sn	Schatten sn	sig n**2	sig m**2	sig s**2	sig nm**2	sig ns**2	sig ms**2	DN	An	Am	As	An*Fn	Am*Fm	As*Fs	Our Flux
1	199.5217391	137.3300000	109.5000000	8.084044697	11.38853224	7.00713922	65.352	129.699	49.100	8476.039	3208.772	6368.205	18053.015	0.353	0.178	0.470	70.381	24.409	51.411	140.20:
2	199.5217391	163.0714288	132.0000000	8.084044697	9.06930984	6.95701085	65.352	82.252	48.400	5375.339	3163.026	3981.018	12519.381	0.318	0.253	0.429	63.448	41.200	58.676	161.32'
3	199.5217391	192.4000000	156.5000000	8.084044697	6.58908188	8.50294067	65.352	43.418	72.300	2837.313	4724.934	3138.977	10701.223	0.293	0.442	0.265	58.525	84.951	41.494	184.97'
4	199.5217391	216.7000000	184.0000000	8.084044697	7.50653049	8.34266145	65.352	56.348	69.600	3682.442	4548.484	3921.821	12152.747	0.323	0.374	0.303	64.388	81.106	55.754	201.24(
5	199.5217391	234.6166667	208.3300000	8.084044697	5.05308487	6.31400550	65.352	25.534	39.867	1668.671	2605.358	1017.942	5291.970	0.192	0.492	0.315	38.379	115.507	65.691	219.67:
6	199.5217391	241.8666667	218.6700000	8.084044697	0.92915734	1.52752524	65.352	0.863	2.333	56.420	152.487	2.014	210.922	0.010	0.723	0.267	1.906	174.859	58.493	235.25:

Figure 4-3. Calculation of the Parameters Used in Linear, Unbiased Minimum-Variance Estimation (6-Month Partition Procedure--Partitioned Average of Data)

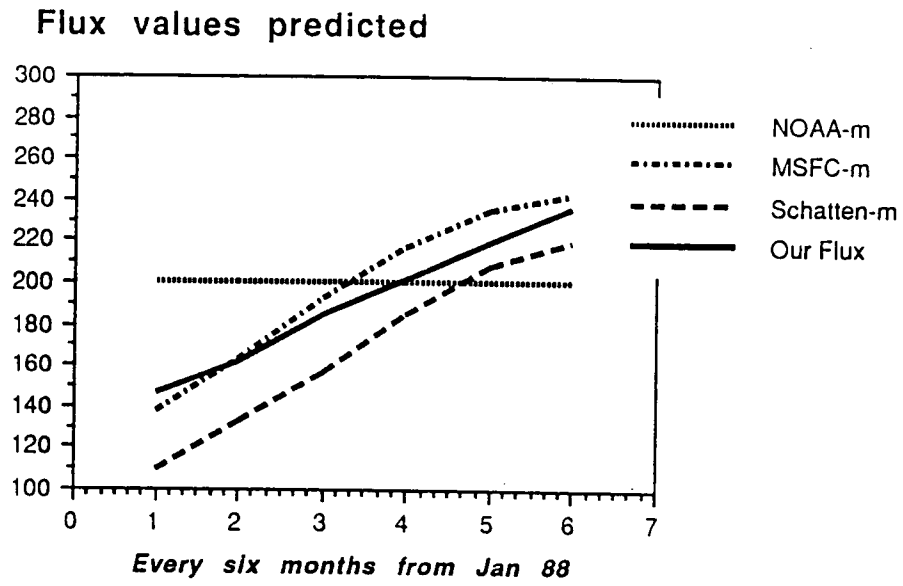

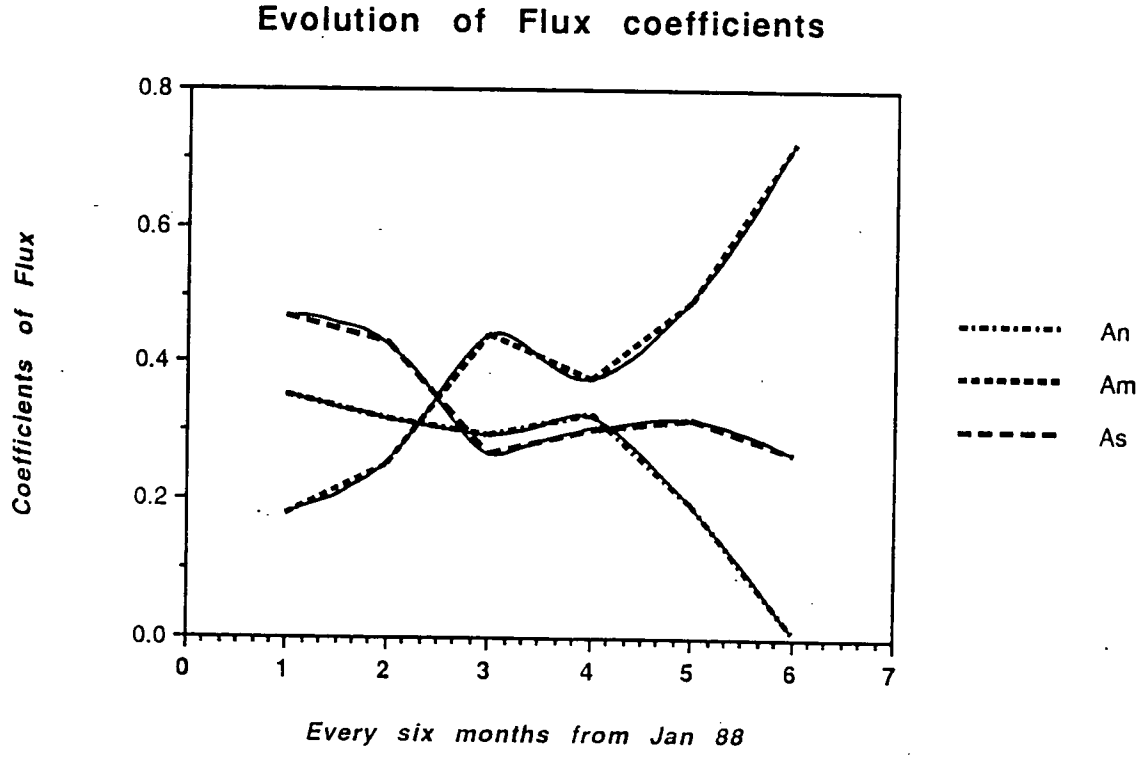

Figure 4-4. Plot of the Predicted Flux by NOAA, MSFC, Schatten (Nominal) and Result of Linear, Unbiased Minimum-Variance Estimation (Time Evolution of the Coefficients a_n, a_m, and a_s--Partitioned Procedure)

6176

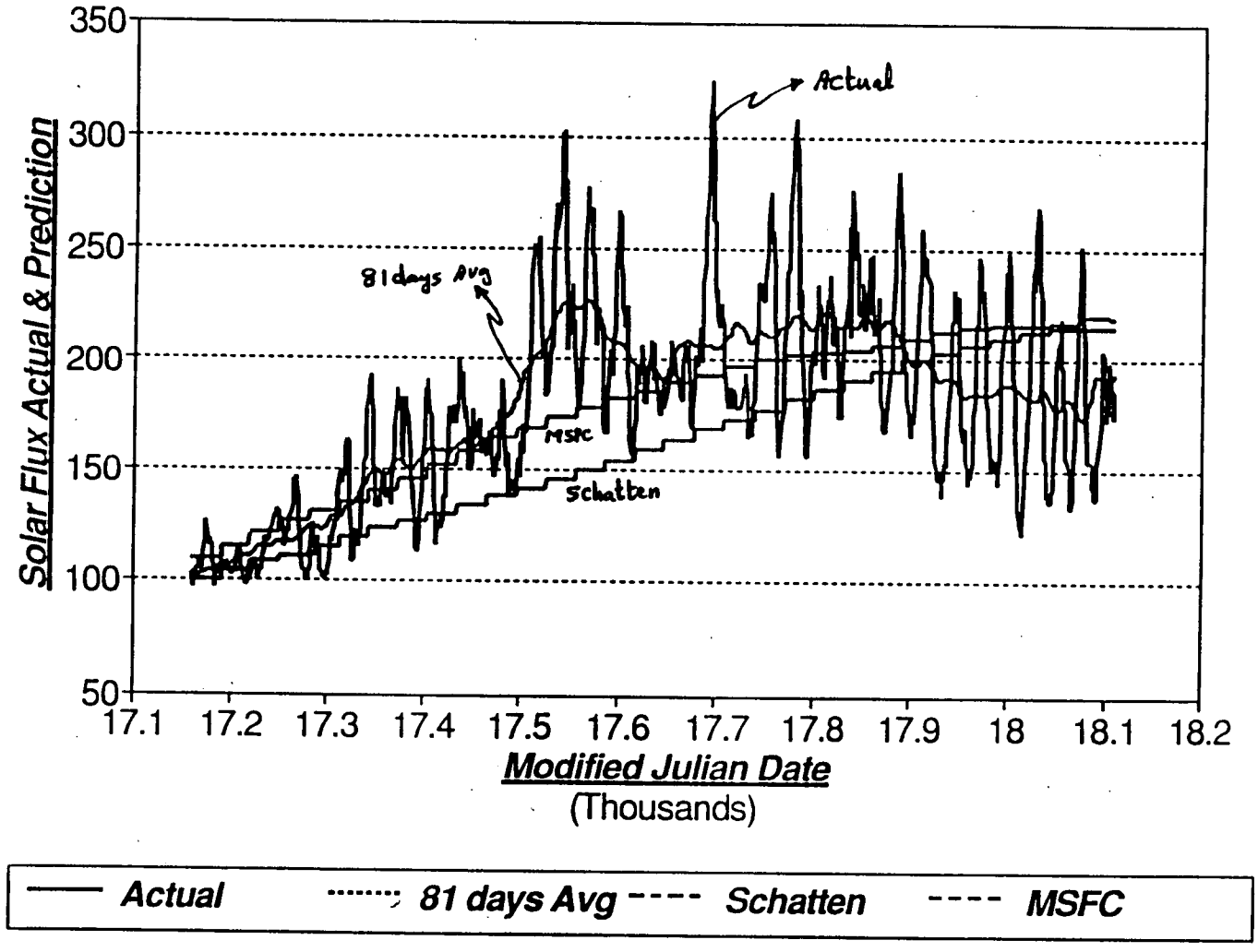

Figure 4-5. Plot of the Actual Solar Flux Values, Nominal Schatten and MSFC Predictions, and 81-Day Average

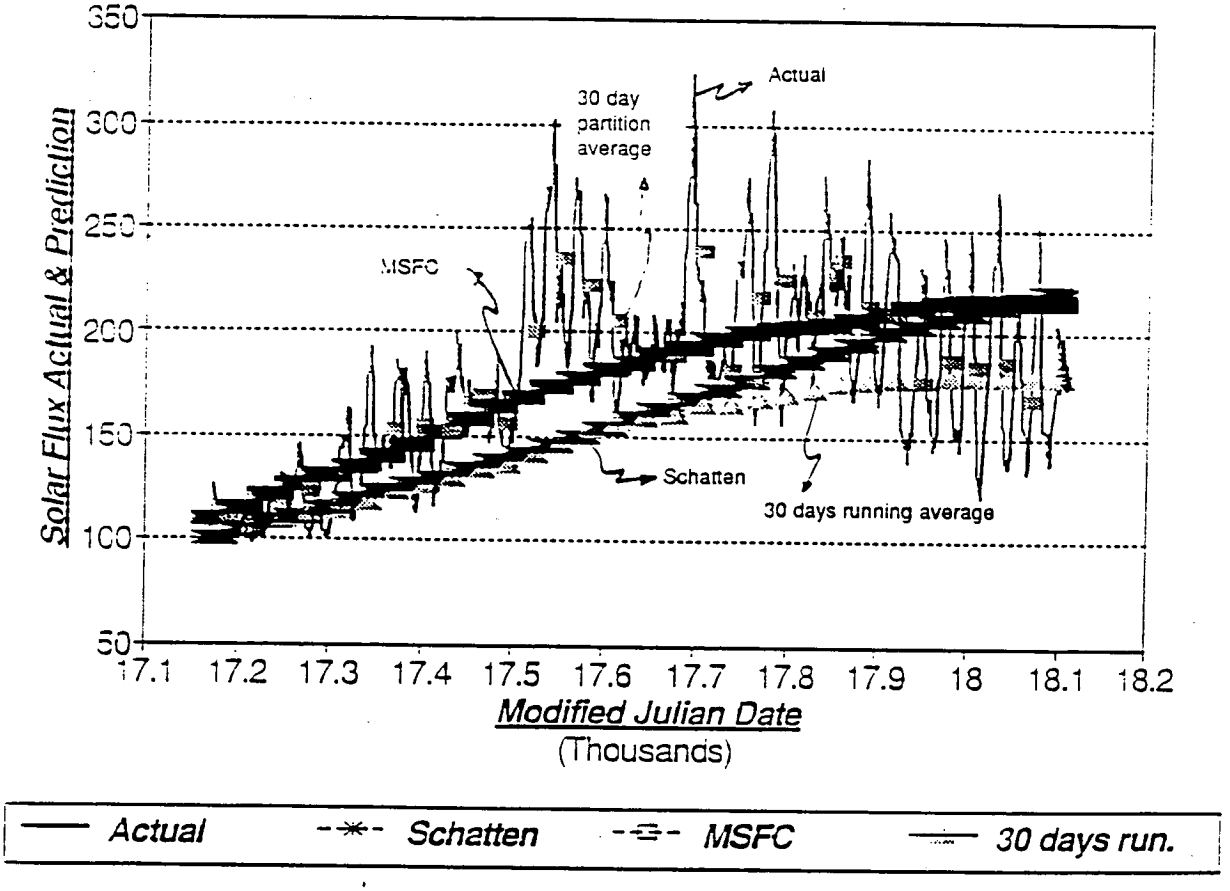

Figure 4-6. Plot of the Actual Solar Flux Values, Schatten, and MSFC Predictions With 30-Day Running Average and 30-Day Partitioned Average

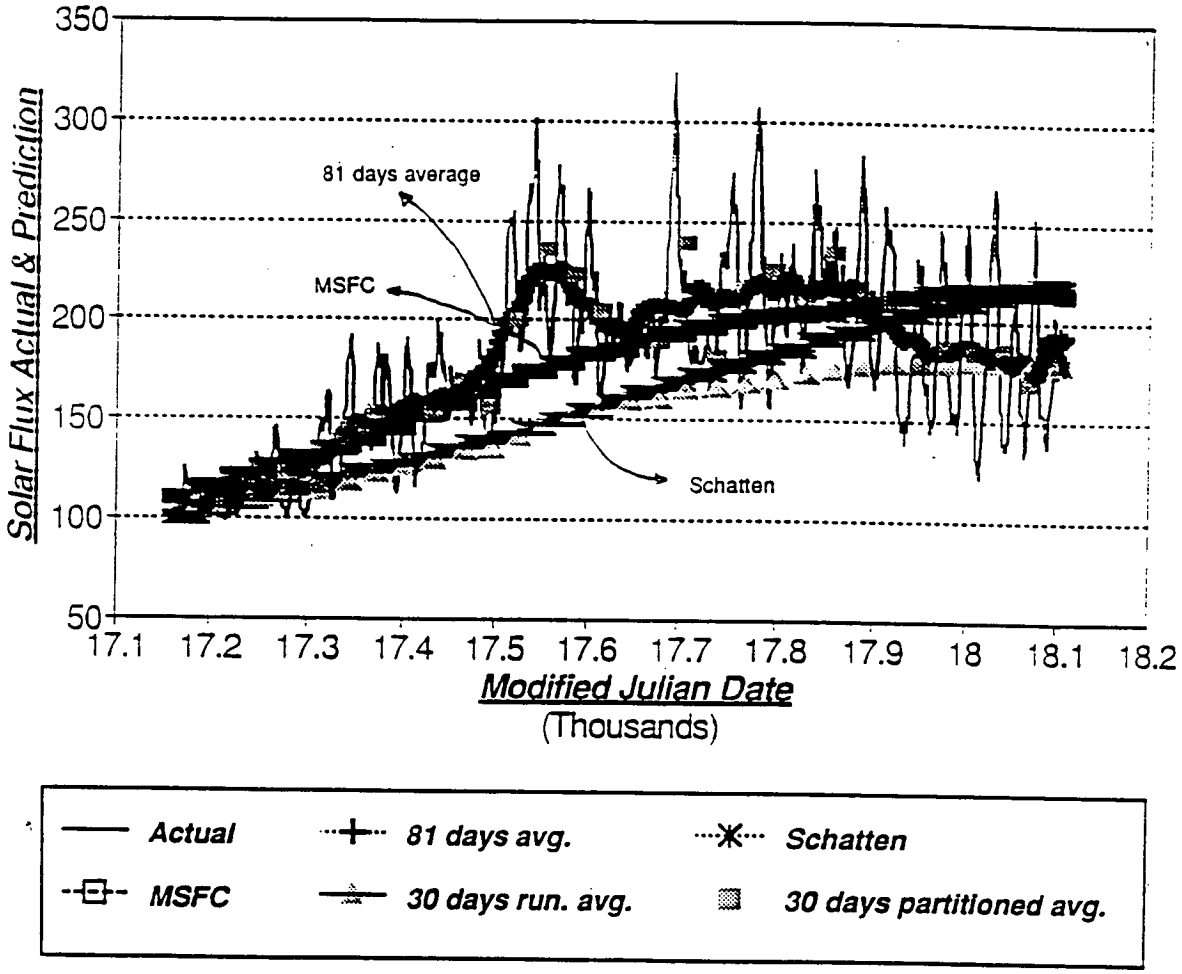

Figure 4-7. Plot of the Actual Solar Flux Values, Schatten, MSFC Predictions, and 81-Day Average With 30-Day Running Average and 30-Day Partitioned Average

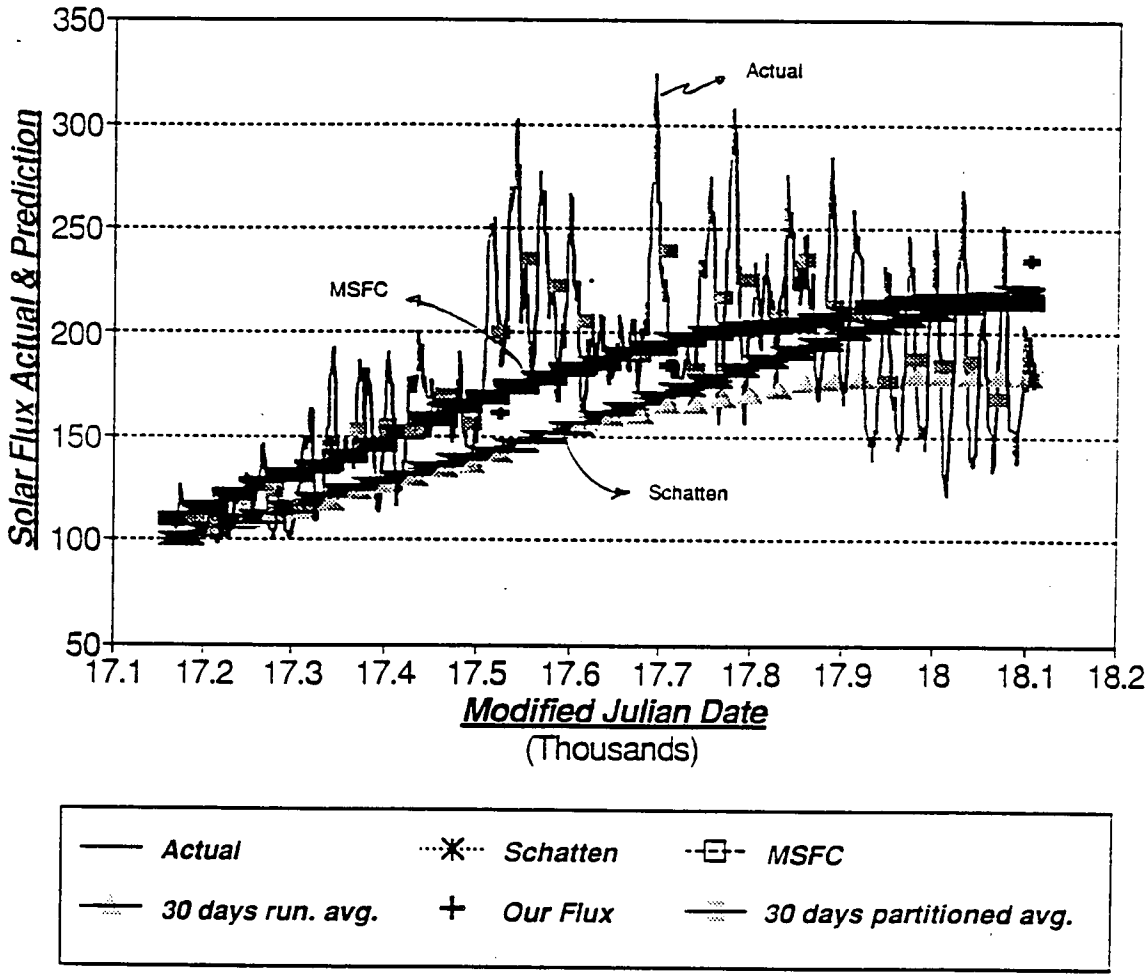

Figure 4-8. Plot of the Actual Solar Flux Values, Schatten, and MSFC Predictions (30-Day Running Average; 30-Day Partitioned Average; and Linear, Unbiased Minimum-Variance Estimation by 6-Month Partitioned Procedure)

6176

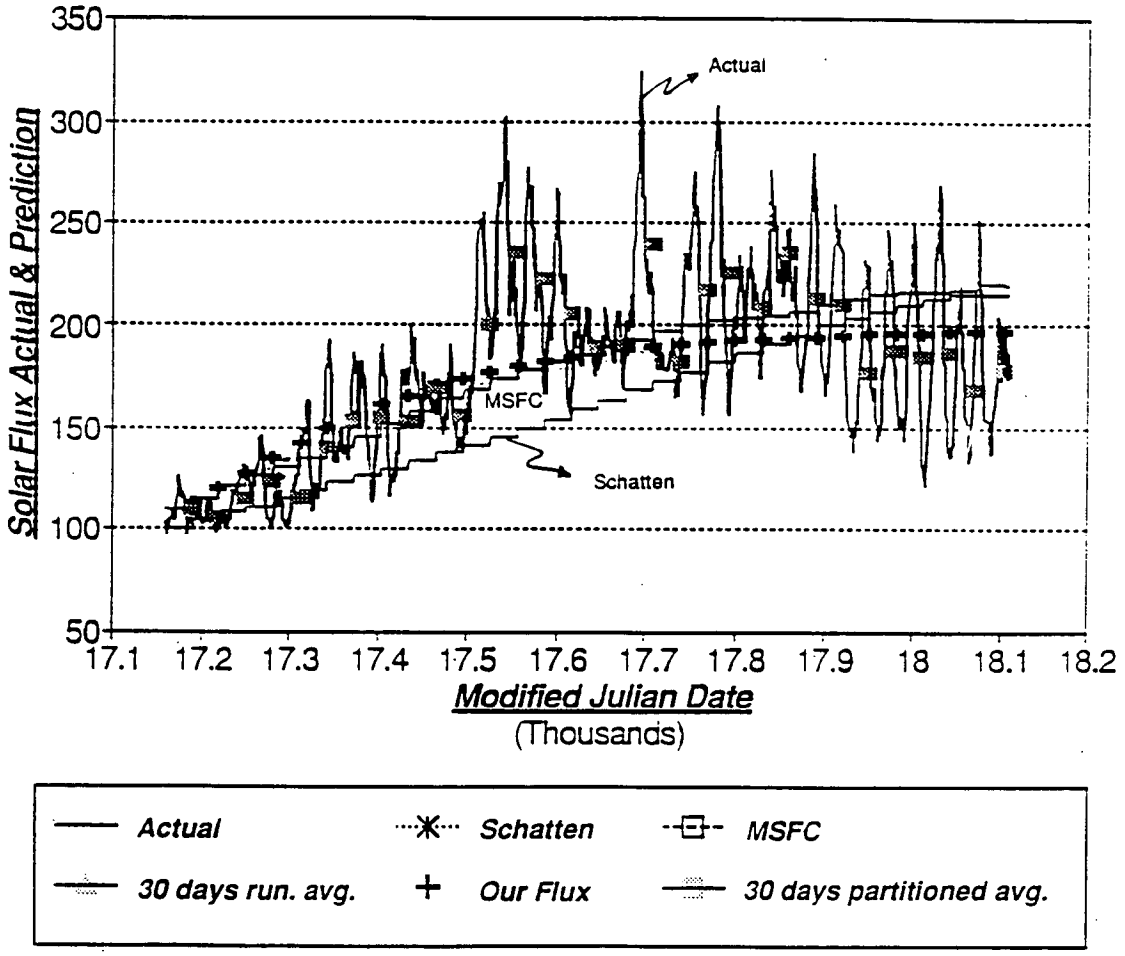

Figure 4-9. Plot of the Actual Solar Flux Values and the Schatten and MSFC Predictions With 30-Day Running Average and the Estimated Combined Flux With Partitioned Procedure

6176

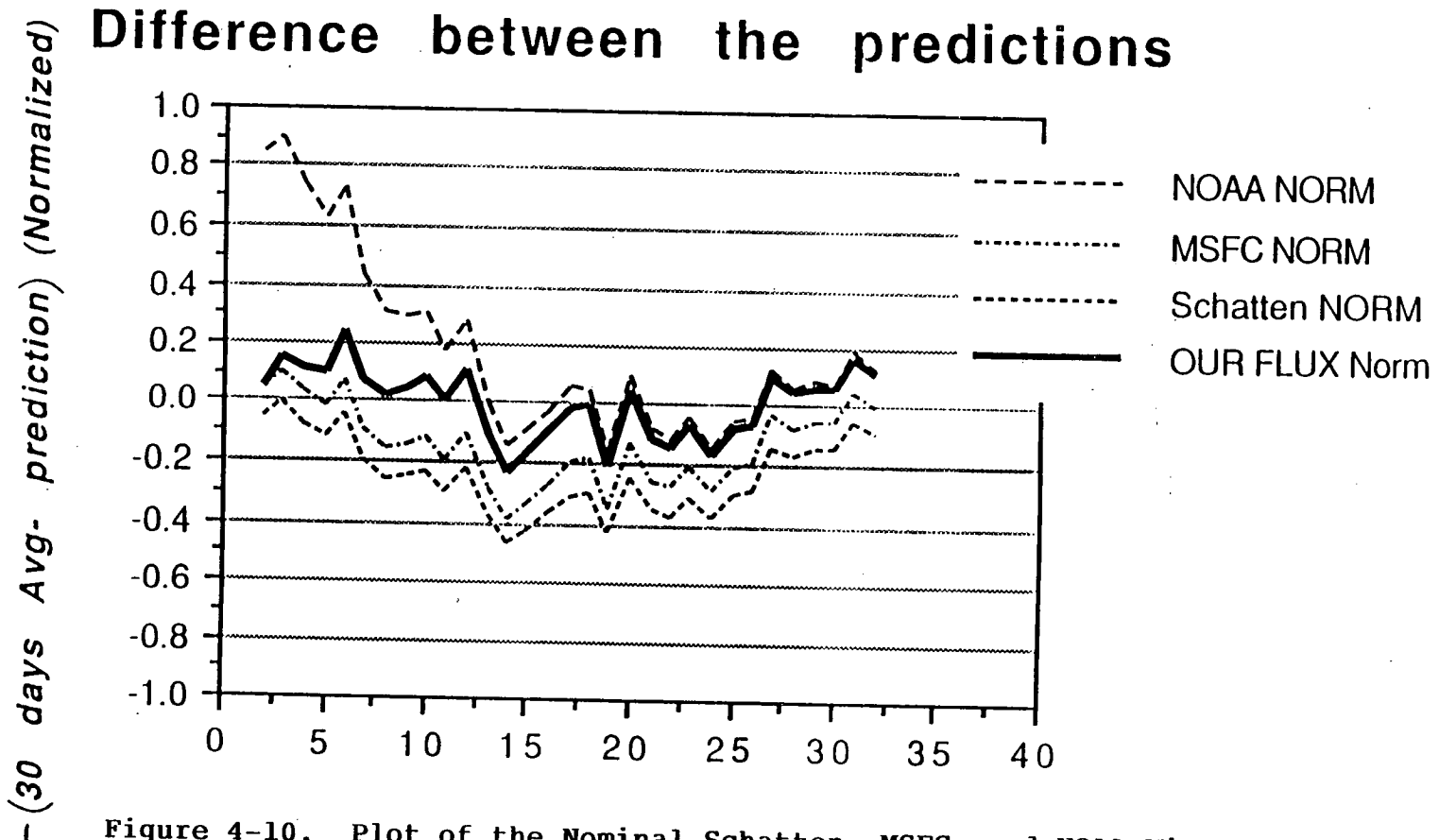

Figure 4-10. Plot of the Nominal Schatten, MSFC, and NOAA Minus 30-Day Average of Actual Values and Linear, Unbiased Minimum-Variance Estimation (Normalized)

Finally the combined flux is calculated from Equation (4-21). Note that these equations require variances of NOAA, MSFC, and Schatten data that had been calculated using the Quattro Pro program.

The time evolutions of a_n, a_m, and a_s are presented in Figures 4-2 through 4-4, which indicate that their variations are not violent and are predictable in a sense. Figures 4-5 through 4-8 present the actual solar flux values for a period of 2 years with MSFC and Schatten predictions and different kinds of averages, so that one can clearly see that MSFC predictions are closer to the actual values than Schatten predictions. Figure 4-9 presents the combined flux values, which are better than all the other models, because it apparently has all the inherent physics of the individual models built into it by the proper coefficients (a_n, a_m, and a_s). Figure 4-10 presents the normalized deviations of the predictions by individual models from the 30-day average of the actual solar flux values. It is clear from this graph that the combined solar flux prediction model varies within 20 percent of the actual values, whereas the other individual prediction models show variations much larger than 20 percent from the actual values.

SECTION 5 - CONCLUSIONS AND RECOMMENDATIONS

The statistical analysis using confidence intervals reveals that one cannot draw a general conclusion about which solar flux forecast model is better than the others among Schatten, NOAA, and MSFC. This is due to the fact that these models assume stochasticity (structurally random) in solar flux time series, which is chaotic (existence of an underlying structure in data).

Before employing the nonlinear, chaotic approach that will follow as the second sequence of the analysis (to be published in a different document), a combined LUMVE has been developed that properly combines all three models into one that minimizes the variance. All the physics inherent in each model are combined.

In the second part of these studies, solar flux as a chaotic time series will be studied and a particular route through which the dynamical time series becomes chaotic will be identified. The third part of the sequence is a critical stochastic approach to solar flux. In this part solar flux is studied through model identification, estimation, fitting, diagnostic checking, and mathematical forecasting for solar flux chaotic data.

The following future investigations are recommended:

- A Box-Jenkins type approach to solar flux time series model identification, estimation, fitting, diagnostic checking, and forecasting of solar flux. This is a method to classify the solar flux time series as one of the presently known models (moving average (MA) model, auto regressive (AR) model, and mixed auto regressive moving average (ARMA) model). Once the classification is made, proper forecastings seem possible.

- Chaotic approach to solar flux prediction. Since solar flux is shown to be chaotic, this approach would allow for the construction of an iterative manifold that can reconstruct the solar flux time series. To do this a sequence of studies should be performed such as

  - Finding Lyapunov spectrum from solar flux time series (Reference 11)
  - Forming attractors from solar flux time series and nonlinear signal processing using Neural Net
  - Extracting self similarity character and fractal structures from solar flux time series and modeling abrupt changes with Thom's elementary catastrophes (Reference 12)

REFERENCES

1. Schatten Forecasts of Solar Flux, NASA, GSFC, Greenbelt, MD, electronic message

2. MSFC Forecasts of Solar Flux, NASA MSFC, Huntsville, Alabama, electronic message

3. NOAA Forecasts of Solar Flux, NOAA, Boulder, Colorado, electronic message

4. J. C. Brandt, Introduction to Solar Wind, W. H. Freeman and Company, 1970

5. G. Gamow, A Star Called the Sun, Viking Press, 1964

6. I. Oh, The Average Solar Flux (10.7cm) Model for an 11-Year Solar Cycle, prepared for NASA GSFC (NAS-5-11933MOD13), September 1974

7. J. S. Bendat and Allan G. Piersol, Random Data, John Wiley & Sons, 1971

8. Donald B. Owen, Handbook of Statistical Tables, Addison-Wesley Publishing, 1962

9. Goddard Space Flight Center, Flight Dynamics Division, FDD/554-91/006, Future Mission Studies on Solar Flux Analysis, S. Ashrafi, prepared by Computer Sciences Corporation, December 1990

10. Solyman Ashrafi, Evidence of Chaotic Pattern in Solar Flux Through a Reproducible Sequence of Period-Doubling Type Bifurcations, Proceedings of Flight Mechanics/ Estimation Theory Symposium, May 1991

11. --, Existence of a Time Horizon for "Structural Stability" and "Computability" To Become Formally Incompatible in Prediction of Solar Flux (in preparation)

12. --, Towards Modeling the Formation of Abrupt Changes in Solar Flux by Thom's Catastrophe Theory (in preparation)

DISTRIBUTION LIST

<u>GSFC</u>
J. Cooley
M. Saltzberg
J. Teles
FDD CMO